Heliyon 8 (2022) e09711

Contents lists available at ScienceDirect

Heliyon

journal homepage: www.cell.com/heliyon

Research article

Impact of climate change on future precipitation amounts, seasonal distribution, and streamflow in the Omo-Gibe basin, Ethiopia

Tamiru Paulos Orkodjo [a,*], Gordana Kranjac-Berisavijevic [b], Felix K. Abagale [c]

[a] Faculty of Hydraulic and Water Resource Engineering, Insititute of Arba Minch Water Technology, Arba Minch University, Ethiopia
[b] Department of Agricultural Mechanisation & Irrigation Technology Faculty of Agriculture and Consumer Sciences, UDS, PO Box 1882, Nyankpala, Ghana
[c] Department of Environment, Water and Waste Engineering, School of Engineering, University for Development Studies, Tamale, Ghana

ARTICLE INFO

Keywords:
Climate change
RCM
Precipitation
Streamflow
SWAT
Omo-Gibe
Ethiopia

ABSTRACT

This study projected the impact of climate change on the amount of precipitation, seasonal distribution, and streamflow of the Omo-gibe basin, Ethiopia. Projections of climate change using the results of high-resolution multimodal ensembles from fifteen regional climate models (RCMs) of the Coordinated Regional Climate Reduction Experiment (CORDEX)-Africa were statistically downscaled and bias-adjusted using a quantile mapping approach. Precipitation and temperature were projected under RCP 8.5 and RCP 4.5 emission scenarios. Climate and streamflow projections from a mean ensemble of RCMs in the near future (2025–2050), medium future (2051–2075), and far future (2076–2100) were compared to the reference (1989–2019). Mann-Kendall (MK) trend testing was used to determine if a change is statistically significant and to detect trends in temperature, precipitation, and streamflow. The Soil and Water Assessment Tool (SWAT) hydrological model was used to project the impact of climate change on the streamflow. According to RCP4.5 and RCP8.5, the emission scenarios predicted significant positive (rising) temperature, but significant negative (decreasing) precipitation and streamflow. The average temperature projected increases range from 2.40-3.34 °C under the RCP 4.5 emission scenarios and 2.6–4.54 °C under the RCP 8.5 emission scenarios. Annual average precipitation projected decreases range between 10.77-13.11% under the RCP 4.5 emission scenario, while the RCP 8.5 emission scenarios decrease range between 11.10-13.86% in the rainy summer season (June–August) and the irregular rain season (March–May). Projected annual average streamflow decrease range between 7.08-10.99% under the RCP 4.5 emission scenarios and 10.98–12.88% under the RCP 8.5 emission scenarios. Results on projected temperature increases and reductions in precipitation and streamflow will help to develop effective adaptation measures to reduce the ongoing impacts of climate change and draw up long-term water resource management plans in the river basin. Both the results and the multidisciplinary approach will be vital to irrigation and hydropower project planners.

1. Introduction

Globally and regionally, temperatures are projected to increase in the coming decades (Immerzeel et al., 2012; Seager et al., 2013; Sorg et al., 2012; Wu et al., 2012; Yang et al., 2014). According to various climate model simulations, the average temperature of our planet at the end of 21 century could be 1.1 to 5.4 °C (2–9.7 °F) higher than it is today (Solomon et al., 2007; Friedlingstein, 2010). This is due to carbon dioxide and other 'greenhouse' gases, which trap heat produced by human activities by releasing carbon dioxide into the Earth's atmosphere and increasing greenhouse gas emissions effect (IPCC, 2007; Hegerl et al., 2007; IPCC, 2013; IPCC, 2014; Shamir et al., 2015). This increasing concentration of greenhouse gases (GHGs) in the Earth's atmosphere is expected to contribute to global climate change. This situation has the potential to alter the global and regional hydrological cycle, as well as the frequency and amount of precipitation (IPCC, 2012; IPCC, 2013). It can also alter the spatial and temporal distribution of critical hydrological conditions and processes (Kumar et al., 2017) and lengthen the dry season, leading to drought, sea-level rise, and frequent flooding (Giorgi et al., 2009), as well as water stress and scarcity (Arnell et al., 2013). Global and regional climate change will also impact the amount, distribution of annual and seasonal precipitation (Giorgi et al., 2011), the magnitude of streamflow, and water availability (Elsner et al., 2010; Hamlet et al., 2013), as well as soil moisture and evapotranspiration.

* Corresponding author.
E-mail addresses: tamirupaulos@gmail.com, tamiru.paulos@amu.edu.et (T.P. Orkodjo).

https://doi.org/10.1016/j.heliyon.2022.e09711
Received 22 October 2021; Received in revised form 18 December 2021; Accepted 7 June 2022

Climate change has had a significant impact on precipitation, temperature, and streamflows across the river basins, regionally and worldwide. The trend analysis of these meteorological and hydrological variables has received a lot of attention to aid the prediction of change, and management of water resources for a variety of sectors and uses (Ahmad et al., 2015). Understanding these hydroclimatic variables regardless of whether a change is statistically significant or not and detecting trends in changes due to the future impact of climate change is necessary to assess both long-term and short-term trends in temperature, precipitation, and streamflow data. It is also vital to examine the river basin's streamflow as well as water availability in the present and future. At the scale of the river basin, the spatial and temporal distribution of temperature, precipitation, and the assessment of streamflow trends detection is also essential for the development and management of water resources, the long-term economic development, and assessment of the future impact and behavior of climate change.

Global Climate Models (GCMs) are constantly improving, and even the most recent generation of several Coupled Model Intercomparison Project Phase 5 (CMIP5) multi-model ensembles models (Tayler et al., 2012) are becoming available. These models have been developed to estimate and project climate change, increase in greenhouse gas concentrations, and climate variables in the climate change scenarios provided by the Intergovernmental Panel on Climate Change (IPCC) in its Fifth Assessment Report (AR5) (IPCC, 2013; IPPC, 2014). The models are tools for assessing and estimating the impact of climate change at regional and global levels. The models used a set of four new climate scenarios known as Representative Concentration Paths (RCPs) to project climate variables and change (Moss et al., 2010; van Vuuren et al., 2011). These scenarios were designed for the climate change assessment and modeling community as a foundation for long- and short-term climate change assessment and modeling investigations by the year 2100. Scenarios of radiative forcing values in the range of 2.6–8.5 W/m^2 in the year 2100.

The Omo-Gibe River is one of Ethiopia's most important river systems with three cascading dams, Gilgal Gibe I, Gibe II, and Gibe III, which supply 45% of the country's hydroelectric power. Over the last decade, climate change has created water constraints in the Omo-Gibe River basin for hydropower production and other uses. According to the Ethiopian government, the Gibe III dam on the Omo-Gibe River Basin caused a 476-megawatt energy deficit because of the impact of climate change, which was announced in May 2019. Therefore, it is vital to predict and quantify how future climate change will affect the amount and frequency of precipitation, seasonal distribution, and magnitude of streamflow in the Omo-Gibe River basin.

The objective of this study was to estimate and project the potential impacts of climate change on the future amount of rainfall, seasonal distribution, and streamflow of the Omo-Gibe River. This is based on precipitation and temperature projections under the RCP 4.5 and 8.5 climate change scenarios using a multi-model ensemble of GCMs to RCMs models statistical downscaled and quantile mapping bias-corrected climate data. Streamflow simulation and projection using RCMs models produce data as input for the Soil Water Assessment Tool (SWAT) hydrological model. Whether a change is statistically significant and to detect a change in trend in hydroclimatic variables due to future impacts of climate change by applying the Mann- Kendall (MK) trend test.

Understanding the impacts of future climate change on precipitation, seasonal distribution, and streamflow is key to developing appropriate and effective climate change adaptation strategies. It is also needed for effective water resource management in the future, long-term water resource sustainability, and climate change mitigation and adaptation options. This enables planners, politicians, legislators, and policymakers, as well as water managers, river basin planners, government agencies, river basin administrations, and engineers to make better decisions and plan future projects to mitigate the future effects of climate change within the basin.

2. Materials and methods

2.1. Study area

The Omo-Gibe River basin lies in southwestern Ethiopia, with geographic coordinates ranging from 4°30′ to 9°30′ N and 35° to 38°E. An estimated 14,580,516 people live along the Omo-Gibe River (Central Statistics Agency, 2017). The Omo-Gibe River flows into Lake Turkana, Kenya, with an area of drainage of approximately 79,000 km^2 (Figure 1). The basin also includes parts of the Oromia region. The uplands cover 51% of the basin, with a mean altitude of 2800 m above sea level (a.s.l). Annual precipitation varies between 1900 mm/year in the uplands and under 400 mm/year in southern lowlands. The mean annual air temperature of the basin is between 23 °C and 17 °C in the west highlands and above 29 °C in the southern lowlands (Woodroofe et al., 1996; Degefu and Bewket, 2014). In addition, the basin has two precipitation regimes: the north and central part are unimodal, with only one peak of precipitation (i.e. without alternating wet and dry months during the rainy season), and the south is bimodal, with two peaks of precipitation. In the Omo-Gibe River basin (June–August) summer has a high rainy season, autumn and winter are mainly dry and hot and spring has an erratic rainy season. The total average annual flow of the basin is estimated to be 16.9 billion cubic meters (FAO, 2016), or 14% of the country's annual surface water resources (Woodroofe et al., 1996). The topography of the basin is varied and distributed among the plateaus of the north and center of the basin, with altitudes greater than 1500 m above sea level (m.a.s.l) and a maximum height of 3,360 m.a.s.l (between the Gilgel, Gibe, and Gojeb tributaries). The other portion is the lower plain of Omo, between 400 and 500 m a.s.l (Woodroofe et al., 1996; Worku et al., 2014). There is also significant hydropower and irrigation potential in the basin.

2.2. Data for the study

2.2.1. Geospatial data

To simulate streamflow, the SWAT model requires geospatial input data, including the Digital Elevation Model (DEM) a map of land use and land cover, and a soil map. A digital DEM was used to delineate, create flow lines and extract flow direction and accumulation and sub-basin parameters, and compute sub-basin attributes. DEM data for the basin has been uploaded at a resolution of 30 m × 30 m at https://glovis.usgs.gov/app (Figure 2(a)). A digital map of land use and land cover was used to reflect the heterogeneity of the river basin. The model requires land-use and land-cover cover types to build land-use databases, generate land-use properties, and simulate streamflow. There were thirteen dominant land-use/land cover types in the river basin (Figure 2(b)). A map of land use and land cover types was obtained from Ethiopia's Ministry of Water, Irrigation, and Electricity (MoWIE). A soil map was used to prepare soil databases to extract soil categories, generate soil chemical and physical properties, and stimulate the streamflow. A digital soil map was used to account for the heterogeneity of the drainage basin. There were thirteen dominant soil types in the river basin (Figure 2 (c)). A soil map was obtained from (MoWIE).

2.2.2. Hydro-meteorological data

In this study, observed daily weather data on precipitation, maximum and minimum temperatures, humidity, wind speed, and sunshine from 1980 to 2019 were collected from the Ethiopian National Meteorological Agency (NMA). These climate data are needed to assess the future impact of climate change and are needed for the SWAT hydrological model to simulate streamflow for the reference period. It is also important to compare production in future periods. Daily basin flow data (1986–2018) is provided by MoWIE. It needs model calibration and validation for the baseline period and a comparison of future flow periods.

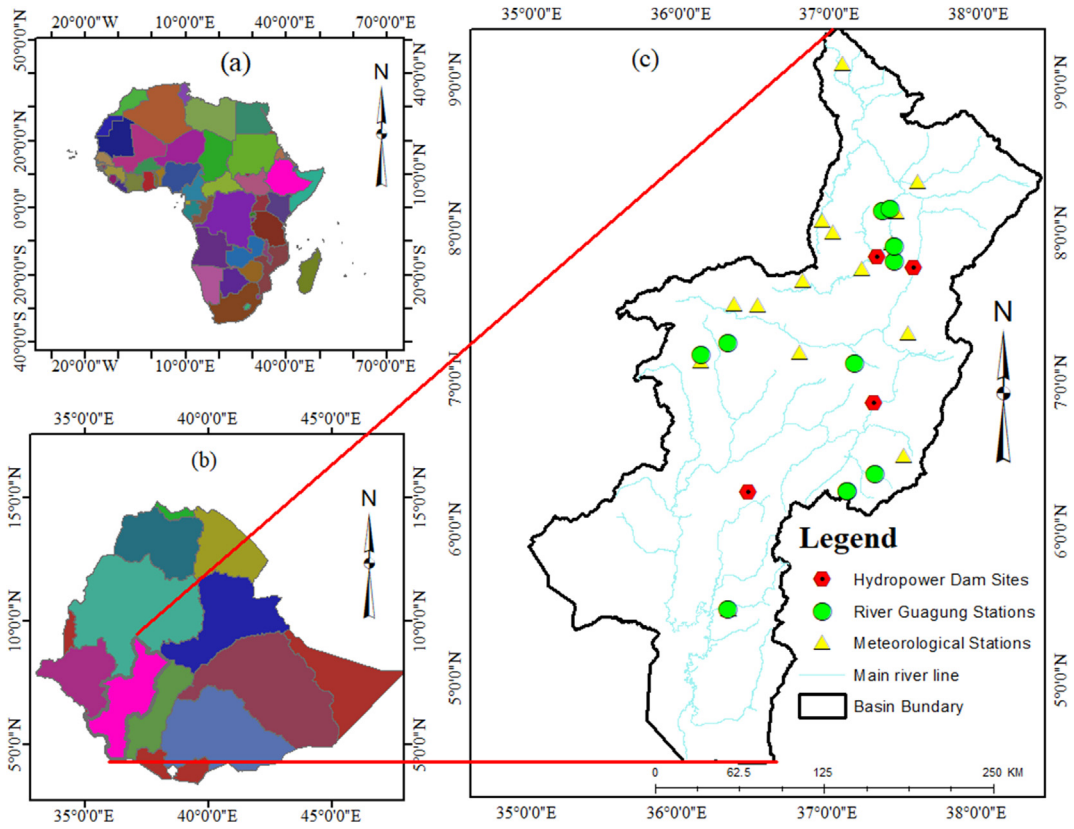

Figure 1. Location of the study area map (a) Africa map (b) Ethiopia's major river Basins and (c) Omo Gibe River Basin.

2.3. Global climate change models (GCMs) and climate data projections

In this study, eleven GCMs models and fifteen multi-model RCMs ensemble models from the Phase 5 Coupled Model Intercomparison (CMIP5) project were used for future climate change projections and assessments under two PCR 4.5 and PCR 8.5 emission scenarios for the Omo-Gibe River basin. To reduce uncertainty and enhance the credibility of climate change projections and impact assessments, the IPCC recommended using the multi-modal ensemble model (MSE) (Knutti et al., 2010). This is crucial for developing countries like Ethiopia, with limited human and natural resources, as well as for effective water supply management in the future. Repository driving GCMs models including CCCma-CanESM2, CNRM-CERFACS-CNRM-CM5, CSIRO-QCCCE-CS IRO-Mk3-6-0, ICHEC-EC-EARTH, IPSL-IPSL-CM5A-LR, IPSL-IPSL-C-M5A-MR, MPI-M-MPI-ESM-LR, MIROC-MIROC5, MOHC-HadGEM2-ES, NOAA-GFDL-GFDL-ESM2M, and NorESM1-M (CMIP5; Tayler et al., 2012). GCM to RCM the statistical downscaling method was utilized to project climate as a part of the CORDEX (Coordinated Regional Downscaling Experiment)-Africa project data from CORDEX-Africa were accessed from (https://pcmdi.llnl.gov/mips/cmip5/dataportal.html) uploaded August 2020). These climate models were selected for this study based on earlier studies conducted in Ethiopia (Bekele et al., 2018), the Great Horn of Africa (Osima et al., 2018), and models that have been used in different hydrological research (Angelina et al., 2015; Fabre et al., 2015).

2.4. Climate change scenarios and Representative Concentration Paths (RCPs)

Representative Concentration Paths (RCPs) are new climate change scenarios that are relevant to the climate research community and are based on the emission forcing level until 2100, replacing the Special Emissions Scenario Report (SRES) criterion (IPCC 2013). There are four different scenarios. RCP4.5, RCP6.0, RCP8.5, and RCP2.6, were designed to examine and model the impact of global warming on future socio-economic development, energy, and land use, population growth, technological growth, etc. RCP2.6 is the most optimistic (mitigation) scenario, with very low carbon dioxide concentration levels (van Vuuren et al. 2011, 2011a). It's will reach a maximum radiative forcing peaking at roughly 3.1 W/m^2 by mid-century in 2050 and then declining to 2.6 W/m^2 by 2100 (Van Vuuren et al., 2007a). Two hopeful or stabilization options for the medium term are RCP 4.5 and RCP 6.0. RCP 4. 5 is a stabilization scenario in which radiative forcing is stabilized at 4, 5 W/m^2 shortly after 2100, but not exceeding the long-run radiative forcing target level (Thomson et al., 2011). It stabilizes around 2100, without exceeding the long-run radiative forcing target level (Wise et al., 2009). RCP 6.0 is a stabilization scenario in which the total radiative forcing of 6.0 W/m^2 is stabilized soon after 2100 with no overshoot (Masui et al., 2011), using a variety of technologies and strategies to reduce greenhouse gas emissions (Hijioka et al., 2008). The increase or business as normal most pessimistic emissions scenario, RCP 8.5, is accompanied by increasing greenhouse gas emissions over time. The radiative forcing value reaches a maximum of 8.5 W/m^2, resulting in high greenhouse gas concentration levels (Rajsekhar and Gorelick, 2017; Riahi et al., 2011). These climatic scenarios (Moss et al., 2010; Tayler et al., 2012) illustrate several climates and representative concentration routes, as well as feasible future alternatives based on various assumptions about economic development, population expansion, and energy and land use.

In this study, the RCP4.5 greenhouse gas emissions stabilization scenario and the RCP8.5 higher greenhouse gas emissions scenarios were used to project the maximum and minimum temperatures, precipitation, and climate change. The scenario calculates emissions and concentrations of all GHGs, aerosols, and chemically active gases over time, changes in land use, radiative forcing under various assumptions, and greenhouse gas concentrations in the coming years (IPCC, 2014; Tapiador et al., 2019). RCP 8.5 is an emissions scenario issue comparable to the

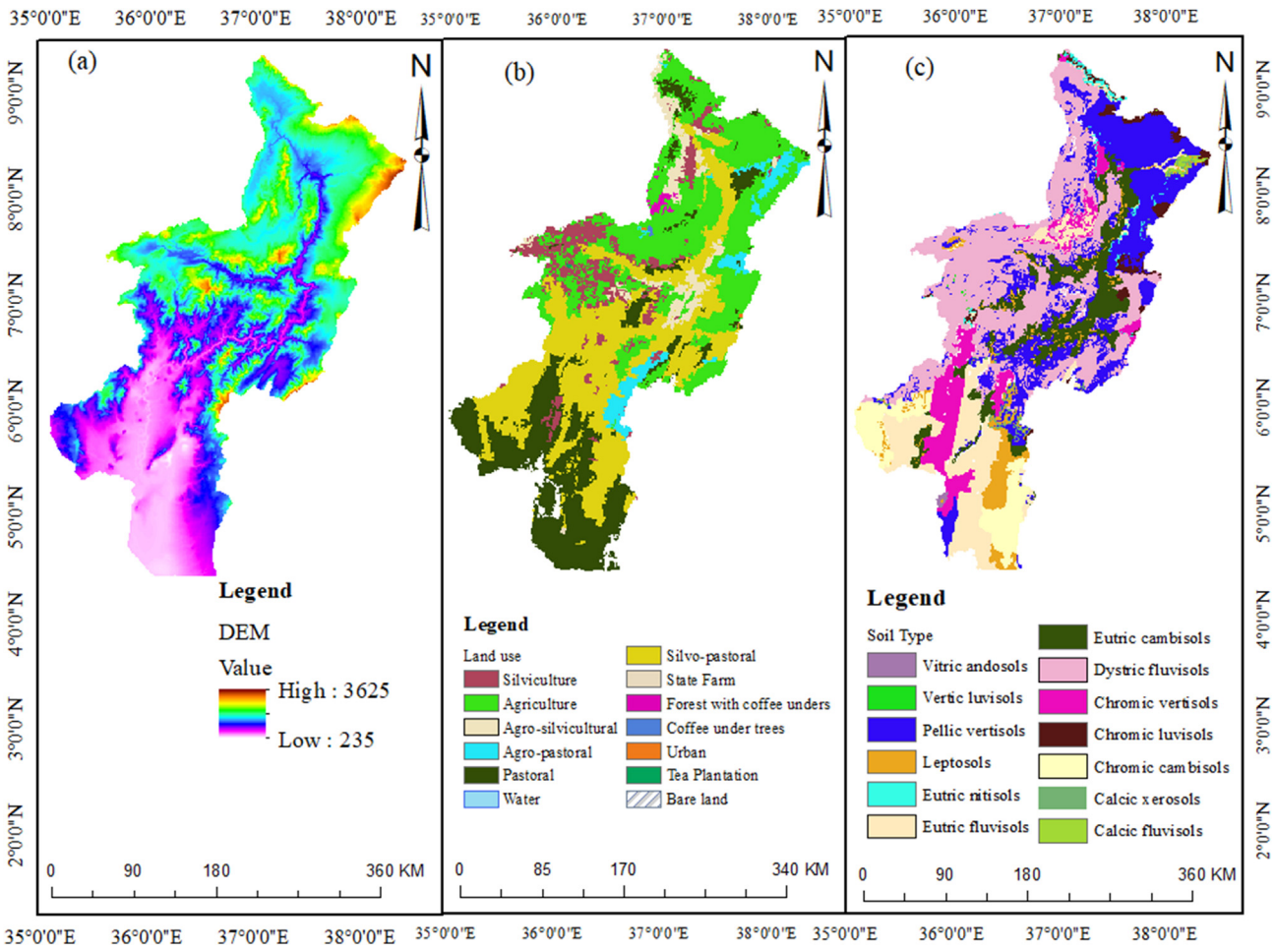

Figure 2. (a) DEM, (b) major land use map types, and (c) major soil types map of the study area.

SRES A2/A1F1 scenario and the business as usual scenario, and RCP 4.5 is an emissions scenario issue equivalent to SRES B an average or stabilizer RCP2.6 scenario does not have an equivalent scenario, and RCP6. 0 in SRES B2 (Tayler et al., 2012). Projected daily maximum and minimum temperatures precipitation and historical were uploaded from the IPCC CMIP5 database distribution center (https://pcmdi.llnl.gov/mips/cmip5/dataportal.html).

2.5. Downscaling of precipitation and temperatures

Estimates, projections, and assessments of future climate change based on GCM data lack geographic and temporal resolutions, as well as regional representation of climate variables. For direct use as hydrological model input and regional-scale climate change impacts assessment studies, the GCM to RCM small scale fine-scale model output is more realistic than the GCM model output (Elsner et al., 2010). To solve this problem, two basic downscaling techniques are commonly used: statistics (Anandhi et al., 2008) and dynamics (Dominguez et al., 2012). Statistical downscaling is based on the relationships between regional climate (predictor) and statistical features of large-scale climate information (predictors), using GCM data as a reference (Acharya et al., 2013; Sachindra et al., 2014a, 2014b), as well as the application of these statistical models to future GCM outputs to derive climate data at a future scale (Wilby et al., 2004). Its downscaling is based on empirical mathematical functions that validate the statistical relationship using variable long-term climate time series data. It is used to generate local climate variables that will remain relatively constant in the future (Wilby and Wigley, 1997; Wilby et al., 2004). The dynamic downscaling method works based on physical realism with complex local processes and relies on nested regional-scale numerical models with higher spatial resolution to simulate finer-scale physical processes and extract consistent and more detailed conditions in small-scale local climates (Abatzoglou and Brown, 2012; Elguindi and Grundstein, 2013; Walton et al., 2015).

In this study, the Delta Statistical Downscaling (DSD) method was used for future regional climate downscaling of temperature and precipitation through the climate project Coordinated Regional Downscaling Experiment (CORDEX)-Africa). This statistical downscaling (SD) method is easier and cheaper to create climate change projections of climate variables with high spatial resolution and small scale for regional applications (Gebrechorkos et al., 2019). Downscaling from GCMs to RCMs is necessary before using GCM model data as input for the hydrological model (Dessu and Melesse, 2013).

2.6. Bias correction of precipitation and temperatures

GCM model output data often has a large bias, which requires correlation to monitor data bias reduction and increase data quality and reliability, and serves as a channel to correlate GCM model outputs to the model hydrology (Hawkins et al., 2013; Gebrechorkos et al., 2019). Before using climate data for climate change impact studies and climate change assessment simulations, biases often need to be corrected (Christensen et al., 2007). RCM model data and observed meteorological variables often exhibit statistical discrepancies, resulting in bias. In this study to correct bias and remove bias from future climate daily data temperature and precipitation data, climate model data for hydrological modeling software (CMhyd) (Rathjens et al., 2016) was utilized. This

model CMhyd software was downloaded from https://swat.tamu.edu/software/. To adjust for the distortion in the precipitation and temperature data projected in this study, the quantile mapping method was adopted. Quantile mapping (QM) approaches are the most acceptable means to fit raw RCM results and the best available alternative. The quantile mapping (QM) bias correction approach is a commonly used method (Yang et al., 2018; Han et al., 2018).

3. The Mann-Kendall (MK) trend test

Analysis of trend changes can be found in many disciplines of meteorology and hydrology, including the identification of trends in precipitation, trend streamflow (Naveendrakumar et al., 2018; Shi et al., 2013), and temperature trend (Amirabadizadeh et al., 2015; Easterling, 1997), streamflow forecast (Kahya and Kalayc, 2004), identification of evaporation trend (Fu et al., 2009) and wind speed trend (Rehman et al., 2012). Trend analysis and verification of current and future changes in any long-term hydroclimatic variable are essential to estimate the future behavior of climate change due to increasing greenhouse gas concentrations in the earth's atmosphere.

The two-sided homogeneity test of the R software was used in this study to examine the evolution of the change in trend in the annual and seasonal distribution of precipitation, temperature, and streamflow, as well as to assume levels of significance of the data statistics and of the null hypothesis a reference period (1989–2019) and periods of near future (2025–2050), medium future (2051–2075), and far future (2076–2100). H0 indicates that the data series does not have a monotonic trend, while HA indicates that the data series has a monotonic trend over time. The statistics from the test were compared to the distribution to see whether the null hypothesis should be accepted or rejected. When the absolute value of Z exceeds the critical value (which corresponds to some type of error), the null hypothesis is rejected, keeping the Type I error less than 5% or 10%. Can use tables (standard normal distribution) or software to obtain them for a specific significance level (0.05 or 0.1). With a p-value of (0.05 or 0.1), the critical value of Z 1/2 determined from the standard normal table is 1.96.

The observed and predicted precipitation, temperature, and streamflow trend tests were assessed for these data significance levels using the Z score (standard deviations), p-value (probability), and an absolute value of confidence level -1.96 and +1.96 and 0.05 and 95 percent, respectively. The null hypothesis is accepted if the P-value is less than or equal to 0.05, but if it is greater than 0.05, the null hypothesis is rejected. The statistical significance of observed and projected precipitation, temperature, and simulated and predicted streamflow was determined at a level of 0.05. The mathematical equations used for the standardized calculation of Z-test statistics and time, as well as statistics from the MK (Var [S]) series, calculate the variance for the corrected links (assuming P-value links in the data) using equation (Eq.1) as follows:

$$S = \sum_{i=1}^{n-1} \sum_{j=i+1}^{n} \operatorname{sgn}(x_j - x_i) \tag{1}$$

Where n is the number of data points, xi and xj are the data values in time series i and j (j > i), respectively, and sign (xj – xi) is the sign function as

$$\operatorname{Sgn}(Xi - Xj) = \begin{cases} +1, (x_j - x_i) > 0 \\ 0, (x_j - x_i) = 0 \\ -1, (x_j - x_i) < 1 \end{cases} \tag{2}$$

$$E[S] = 0$$

$$\operatorname{Var}[S] = \frac{\{n(n-1)(2n+5) - \sum_{J=1}^{q} t_p(t_p - 1)(2t_p + 5\}}{18} \tag{3}$$

$$Z_s = \begin{cases} \frac{S-1}{\sqrt{\operatorname{VAR}(S)}}, \ if \ S > 0 \\ 0, \quad if \ S = 0 \\ \frac{S+1}{\sqrt{[\operatorname{VAR}(S)}}, \quad if \ S <= 0 \end{cases} \tag{4}$$

In these equations, X_i and X_j represent the time-series observations in chronological order, n represents the length of the time series, t_p represents the number of ties for the p^{th} value, and q represents the number of tied values. In the hydro-meteorological time series, Z positive values upward trend indicates an increasing trend and negative values downward trend sign indicates a decreasing trend; negative.

Statistical significance of change and to detect changes in temperature, precipitation, and streamflow were assessed using the 'trend' and 'Kendall' software packages R Libraries. This method of pattern detection and analysis is used to determine whether hydrometeorological time series data is increasing, decreasing, or remaining constant over time (R Core Team, 2017). A Github project was used to verify the author's version for all trend detection and assessment, as well as historical time series analysis of trend changes and change points (Patakamuri and Brien 2019; Patakamuri 2019). These CRAN package libraries are publicly available via the CRAN repository and Github version control platform, and they also offer free software downloads as well as full user manuals. Each trend assessment was used to create the interface's mathematical and numerical graphical depiction.

The MK nonparametric trend test method was used in this study to analyze to determine if a change is statistically significant and to detect the trend's significance of hydroclimatic variable changes. It has several advantages, including being less sensitive to outliers, being able to be used for time-series data, and requiring no input data to plot a specific distribution (Ebrahimian et al., 2018; Mondel et al., 2015). It is a simple and widely used nonparametric technique for detecting monotonic upward (upward) and downward (downward) trends, as well as for analyzing the time trend of series data true values, as well as the influence of outliers, and the flexibility of the data to be used, to detect the monotonic trend test and the robust trend test (Repas et al., 2011). This trend test (Mann, 1945; Kendall, 1955, 1975) is the most commonly used approach for detecting annual and seasonal trends in meteorological and hydrological data at the river basin level (Salarijazi et al., 2012; Ejder et al., 2016b; Jain and Kumar, 2012; Anghileri et al., 2014). The approach can also be used to predict the current and future motion of any dynamic changes in hydroclimatic data. It is a technique for determining observed, simulated, and predicted trends in precipitation, temperature, and streamflow by determining whether a trend in the data changes over a time series of meteorological and hydrological variables.

4. Hydrological model soil and Water Assessment Tool (SWAT)

The SWAT model is a conceptual, distributed, process-based, physics-based, multi-purpose, continuous time scale (annual, monthly, and daily), and spatially adapted watershed model that simulates and operates day-to-day, time stages (Arnold et al., 1998, 2012; Neitsch et al., 2011). It is developed by the American Agriculture Organization of the United States (USDA-ARS) department in the early 1990s (Neitsch et al., 2005)). The model was developed to predict the long-term impact of climate and land use management practices on water, water, sediment, yield of water, agricultural chemicals, nutrients cycling, pesticides, nutrients, soil erosion, agricultural management, crop growth, pesticides, bacteria, and agents' pathogens and metals changes in land use and management, in a river basin, of different sizes, topographies, soil types, and land use conditions in large complex basins (Neitsch et al., 2005; Gassman et al., 2007). It simulates and estimates continue over the long-term hydroclimatic variables, as well as the impacts of climate change. SWAT model divides a river basin into several sub-basins, each of

which is subdivided into small hydrological response units (HRUs) with similar land use, slope, soil, and hydrology characteristics (Arnold et al., 2012a; Neitsch, 2011; Singh et al., 2013). This is SWAT's smallest landscaping component, the HRU, which is capable of simulating hydrological processes and cycles in each HRU. The model operates with the Arc Geographic Information Systems (ArcGIS) interface and currently operates with the Q Geographic Information Systems (QGIS).

The model simulates using those methods the surface runoff (Soil Conservation Service, 1972; Green and Ampt., 1911), potential evapotranspiration (Priestley and Taylor, 1972; Penman, 1948; Monteith, 1965; Hargreaves and Samani, 1985), hydrology and hydrological cycle routing phase (William, 1969; Chow, 1964). Interested in SWAT model application, input data, model development, simulation, and estimation methods can find all the necessary information at http://swatmodel.tamu.edu (Neitsch et al., 2005, 2011; Gassman et al., 2007; Arnold et al., 2012b). It is used to simulate daily hydrological processes and cycles at each HRU using a general water balance equation (Eq. 5)

$$SWt = SWo + \sum_{i=1}^{t}\left(R_{day} - Q_{surf} - E_a - W_{seep} - Q_{gw}\right) \quad (5)$$

where SW_t is the final soil water content (mm); SW_0 is the initial soil water content on day i (mm); t is time (days); R_{day} is the amount of precipitation on day I (mm); Q_{surf} is the amount of surface runoff on day I (mm); E_a is the amount of evapotranspiration on day I (mm); W_{seep} is the amount of water entering the vadose zone from the soil profile on day i (mm); $Q_{gw}$is the amount of return flow on day i (mm) (Neitsch et al., 2011).

In this study, the ArcGIS interface ArcSWAT hydrologic model (version 2012) was used to estimate and project the impact of climate change on the future streamflow for both reference and future periods. The SWAT hydrological model was chosen for this study since it is a widely used tool for hydrological modeling, streamflow assessment and modeling, and river basin management (Arabi et al., 2007; Setegn et al., 2010; Chien et al., 2013; Sood et al., 2013). The model has been widely tested for water availability and streamflow estimations all over the world (Santhi et al., 2001), and it has proven to be a useful tool for analyzing the effects of climate change on streamflow at the regional and global levels (Tan al. 2014; Swain and Patra 2019). Another reason was often used to assess the impact of climate change on river basin streamflow, and water availability (Bae et al., 2011; Ficklin et al., 2012; Ficklin et al., 2012, 2012; Bessa Santos et al., 2019; Rivas Tabares et al., 2019).

4.1. SWAT model uncertainty analysis calibration and validation

Uncertainty analysis, model calibration, and validation are essential to effectively apply the SWAT model to climate change impact assessment as the input parameters of the model are process-based and must be maintained within a realistic uncertainty interval. All sources of parameter uncertainty, model structure, model output source uncertainties, and measured data, are calculated in SUFI-2 (AbbAspour, 2014; Abbaspour, 2015). It is considered that the SWAT model inputs rainfall data, land use, soil type, parameters, and observed data SWAT model is linked to the SUFI2 program (Abbaspour, 2015; Dao et al., 2017). Simulation uncertainty is quantified using the 95 percent prediction uncertainty (95PPU), often known as the p-factor. The 95PPU is calculated from the likelihood function of an outcome acquired using Latin hypercube averaging at 2.5 percent and 97.5 percent (Abbaspour and Nazaridoust, 2007). Another technique to measure the robustness of a calibration or uncertainty analysis is to use the r-factor, which is computed by dividing the average thickness of the 95PPU band by the standard error of the observed data. The recommended P-factor and R-factor values are'$>$ 0.7′ and '1.5′, respectively (AbbAspour, 2014; Abbaspour and Nazaridoust, 2007; Abbaspour 2015).

SWAT model Calibration and Uncertainty Programmes (SWAT-CUP) were developed for automatically computing uncertainty analysis and model calibration and validation tools for the SWAT model (Fakult and Kiel, 2015; AbbAspour, 2014; Abbaspour, 2015). It is linked to five different algorithms with the SWAT model Generalized Likelihood Uncertainty Estimation (GLUE), semi-automatic Sequential Uncertainty Fitting Ver-2 (SUFI-2) Particle Swarm Optimization (POS), Parameter Solution (ParaSol), and Mark chain Monte Carlo (MCMC) uncertainty analysis methods for SWAT model results. Details on five techniques can be found in (AbbAspour, 2014; Abbaspour, 2015).

Model calibration is the systematic adjustment and evaluation of the most important and sensitive parameters of the model until the model results match as closely as possible the observable behavior of the system being measured in a basin. Model validation occurs after evaluating the calibration of the model by comparing the field of observation data that was not used in the calibration to the model predictions without changing the parameter values.

In this study, the SUFI-2 algorithm was used for model calibration and validation, as well as for uncertainty analysis. The SUFI-2 approach was adopted for this study because it is widely used and combines numerous objective functions in its uncertainty analysis and calibration procedure. Most SWAT CUP programs use the SUFI-2 algorithm for uncertainty analysis to assess susceptibility, model calibration, and uncertainty, as well as current and future streamflow (Wu and Chen, 2014).

4.2. Hydrological model performance assessment and statistical measures of criteria

SWAT-CUP Sequential Uncertainty Fitting optimization algorithm-developed method was used to perform performance evaluations on the SWAT model (Abbaspour, 2015) in this study. The performance of the SWAT model has been calibrated and validated (Arnold et al., 2012b) and SUFI-2 provides several objective function metrics to analyze the performance of the model in SWAT- CUP). The method developed by the SUFI2 algorithm evaluates perform performance of the SWAT model Abbaspour (2015) and is calibrated and validated (Arnold et al., 2012b). SUFI-2 provides several objective function metrics to quantify model performance in SWAT- CUP. The Nash Sutcliffe coefficient (NS), the coefficient of determination (R^2), and the percent bias (PBIAS) to the standard deviation of the data gathered were employed as performance evaluation measures for this study. Uncertainty programs for SWAT, SWAT CUP, and SUFI2 algorithm performance model in detail are given available at https://swat.tamu.edu/software/swatcup/(Abbaspour, 2015). The statistical values of NS, R^2, and PBIAS, were computed using Eqs. (6), (7), and (8), respectively. The Nash-Sutcliffe efficiency value, which can range from 0 to 1 (Nash and Sutcliffe, 1970), is used to calculate model performance evaluation using Eq. (6)

$$NS = 1 - \frac{\Sigma_i(Q_m - Q_s)2_i}{\Sigma_i(Q_m - Q_s)2} \quad (6)$$

Where, n is the total number of observations, $Q_{o,i}$ and $Q_{s,i}$ are the observed and simulated discharge at the ith observation, respectively, and Q_{mean} is the mean observed data over the simulation period.

Coefficient of determination is used to calculate model performance evaluation using Eq. (7)

$$R^2 = -\frac{[\Sigma_i(Q_m - Q_s)\Sigma_i(Q_m - Q_s)]2}{\Sigma_i(Q_{m,i} - Q_s)2\Sigma_i(Q_{m,i} - Q_s)2} \quad (7)$$

Where Q is discharged, Q_{mi}, and O_s are initially the measured and simulated discharge, respectively.

Model performance evaluation statistical the PBIAS is used to calculate the average tendency of the simulated values to be above or below the observed data values (Gupta et al., 1999). When PBIAS is smaller in size, the model provides better performance. Positive (negative) values

indicate overestimation (underestimation) bias in the model, while zero is the best value (Zhang et al., 2011). A representation of equation PBIAS is shown below Eq. (8).

$$PBIAS = \frac{\sum_{i=1}^{n}(Q_{obs} - Q_{sim})}{\sum_{i=1}^{n} Q_{Obs,i}} * 100 \quad (8)$$

Where Q is discharged, Q_{mi}, and O_s are initially the observed and simulated discharge, respectively. These model performance evaluation criteria indicators were suggested by (Moriasi et al., 2015). SWAT Model performance assessment and statistical measures of criteria were carried out during the calibration, and validation process as presented in (Table 1).

5. Results

5.1. Projected changes in annual and seasonal temperature

Statistically significant, change and detect trends projected annual and seasonal maximum and minimum temperatures change were evaluated. Trend test results revealed baseline and projected annual and seasonal maximum and minimum temperatures statistically significantly positive increasing trends. Baseline fifteen weather gauging stations of the Omo-Gibe Basin maximum and minimum temperatures were analyzed (2019–2019) over 30-years. The annual average and seasonal temperature change were assessed results showed a significant level (0.05) positive increasing trend at the eleven meteorological gauging stations, two meteorological gauging stations' results showed a significant negative decreasing trend, as well as two stations, found no statistically significant monotonic trend change presented in (Figure 3).

The trend test analyzed result that projected the annual minimum and maximum temperatures under RCP8.5 and RCP 4.5 emission scenarios results shows positive increasing trends in the three future periods in the river basin as shown in (Figure 4 and Figure 5) respectively.

Projected annual average maximum and minimum temperatures under RCP4.5 and RCP8.5 emission scenarios were evaluated and compared to the reference period. The projected annual average temperature under RCP4.5 and RCP8.5 emission scenarios results show an increase in the future compared to reference in the three future periods in the river basin shown in (Figure 6).

The baseline seasonal average temperature trend test result showed the eleven meteorological gauging stations a significant positive increasing trend, two meteorological gauging stations' results showed a significant negative decreasing trend, as well as two stations, found no statistically monotonic trend change in seasonal temperature as shown in (Figure 7).

Seasonal temperature projections based on the assessed both RCP8.5 and RCP 4.5 emissions scenarios show a considerable rising trend in the river basin during the three future periods specified in (Figure 8).

Each month minimum and maximum temperature variations were analyzed. In comparison to reference periods, the results showed that both minimum and maximum temperatures are expected to rise in the future under RCP 4.5 and RCP 8.5 emission scenarios. During the hot and dry months, the mean monthly minimum temperature estimated under RCP 4.5 and RCP 8.5 emission scenarios is lower, whereas the mean monthly temperature is higher during the two rainy season months (Figure 9). The mean monthly maximum temperature estimated under RCP 4.5 and RCP 8.5 emission scenarios is greater during the hot and dry months and lower during the two rainy season months (Figure 10).

Table 1. Model performance assessment and statistical measures of criteria.

Performance	NSE	R^2	PBIAS
Very Good	0.75 < NSE ≤1	0.5 < NSE ≤0	PBIAS < ±10
Good	0.65 < NSE ≤0.75	0.5 < NSE ≤0.6	±10 ≤ PBIAS < ±15
Satisfactory	0.5 < NSE ≤0.65	0.6 < RSR ≤0.7	±15 ≤ PBIAS < ±25
Unsatisfactory	NSE ≤0.5	RSR >0.7	PBIAS ≥ ±25

Source (Moriasi et al., 2007).

5.2. Projected changes in annual and seasonal precipitation

Statistically significant, detect trends and projected change of baseline period (1989–2019) over 30-years and future periods 75-years annual and seasonal precipitation change were evaluated and compared with the Baseline period. The baseline period of fifteen rainfall gauging stations of the Omo-Gibe Basin precipitation trend change was analyzed. Annual time series precipitation data patterns change, analyzed results showed a significantly decreasing trend at the eleven meteorological gauging stations in the basin. Trend detection test, on the other hand, found no statistically significant monotonic trend change in annual precipitation at the four meteorological gauging stations are indicated (Figure 11).

Projected annual amount precipitation under RCP4.5 and RCP8.5 emission scenarios in three future study periods trend changes were analyzed. Projected annual amount of precipitation under RCP4.5 and RCP8.5 emission scenarios trend test results depicted significantly decreasing trend shown in (Table 2 and Figure 12).

The baseline period of fifteen rainfall gauging stations of the Omo-Gibe River Basin seasonal precipitation trend change was analyzed. Seasonal precipitation distribution patterns change, results showed a significantly decreasing trend at the eleven meteorological gauging stations. Trend detection test, on the other hand, found no statistically significant monotonic trend change in seasonal distribution precipitation at the four meteorological gauging stations are indicated in (Figure 13).

Projected seasonal precipitation distribution under RCP4.5 and RCP8.5 emission scenarios in three future study periods trend test depicted decreasing trend. This means on another hand in the basin (June–August) summer main rainy season and spring erratic rainy season precipitation projected under RCP4.5 and RCP8.5 emission scenarios assessed decreasing trend shown in (Table 2 and Figure 14).

Projected precipitation changes in the annual amount and seasonal distribution under RCP 4.5 and RCP 8.5 emissions scenarios for three future periods assessed and compared to the reference period of the basin. The results evaluated and quantified in (mm) indicate that the annual quantity and the seasonal distribution of the two rainy seasons during the summer from June to August and the spring from March to May compared to the reference periods will decrease expected (Table 2).

5.3. Calibration and validation of the SWAT model

River basin streamflow is the key hydrologic variable that can be used to simulate the response of components of the basin's hydrologic process and cycle to future climate change. As illustrated in (Table 5) the annual, seasonal, and monthly changes in streamflow were simulated and predicted by the SWAT model. The SWAT model was calibrated using 19 of the most sensitive parameter responses to streamflow magnitude and streamflow-relevant parameters. All parameters relevant to streamflow magnitude change were adapted (Arnold et al., 2012b) These parameters' definitions and names (Mutenyo et al., 2013; Wu et al., 2012b). Streamflow parameters selected for SWAT model calibration names and descriptions are shown in (Table 3).

Calibration and validation of the SWAT model were performed using the average monthly streamflow of the measuring station streamflow data. The model configuration data of years (1989–2019) and two years was kept as the warm-up time, allowing the model to initialize and the system to apply the initial values of the input and output variables of the first state of the model. It is important to recognize that there is no information in the hydrologic model regarding the initial parameters of the simulation. As a result, model a warm-up period is necessary (Li et al., 2015). Streamlow's fifteen-year (1995–2010) and eight-year (2011–2018) periods were used for model calibration and validation,

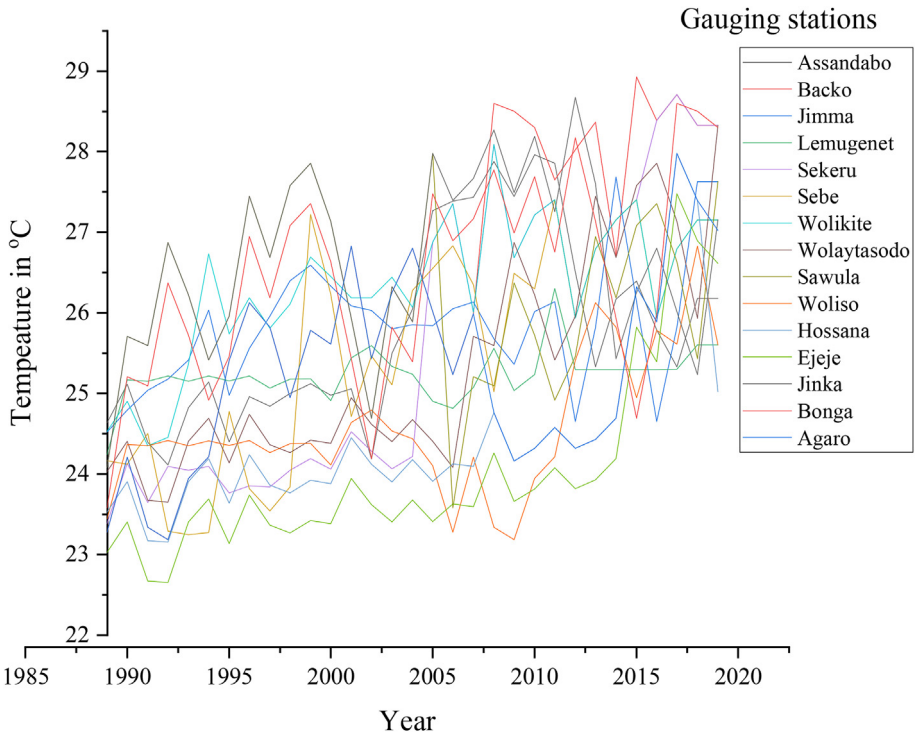

Figure 3. Annual average temperature changes in Omo-Gibe River Basin during (1989–2019).

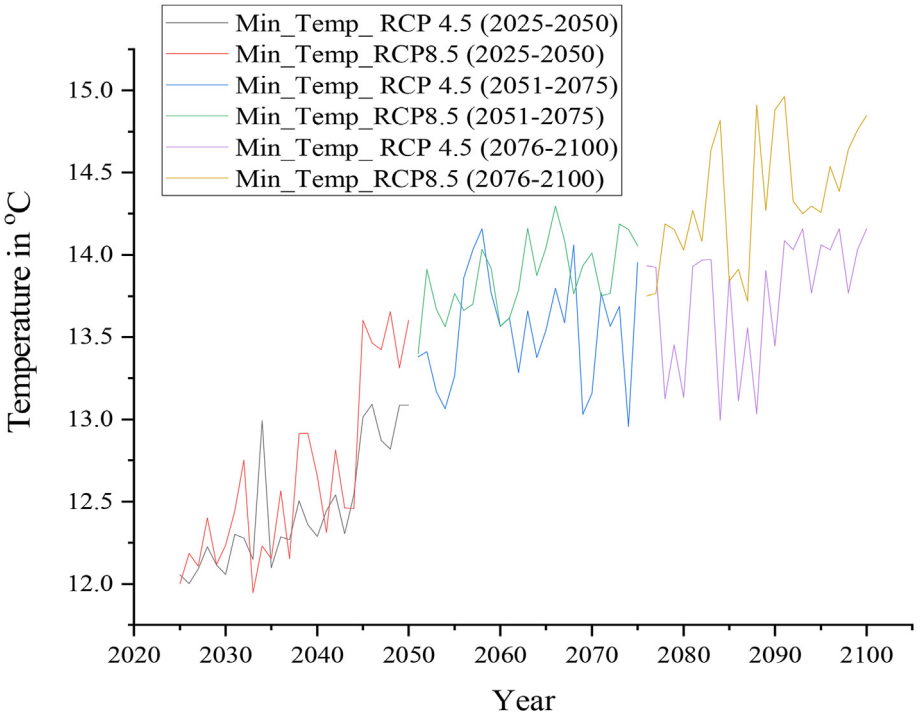

Figure 4. Projected change in annual maximum temperature under RCP4.5 and RCP8.5 emission scenarios during (2025–2100).

respectively. The model calibration was carried out for the period (1995–2010) and the model calibration process was accomplished using the 5,000 simulations of the SUFI-2 algorithm while the validation was carried out for the period (2011–2019). Omo-Gibe River basin measured observed monthly average streamflow at a gauge located at Great Abilite station was used for the calibration and validation period. Model calibration and validation were performed using distinct years of observed monthly mean streamflow data of gauge station measured the observed dry and wet season streamflow was used for the calibration and validation periods. For the calibration and validation periods, the monthly streamflow based on the observed and simulated data at the station corresponded well to the performance evaluation statistics of the R^2, NSE, and PBIAS models and the results of the model are acceptable. The values of the P and R factors suggest that the simulated predictions were

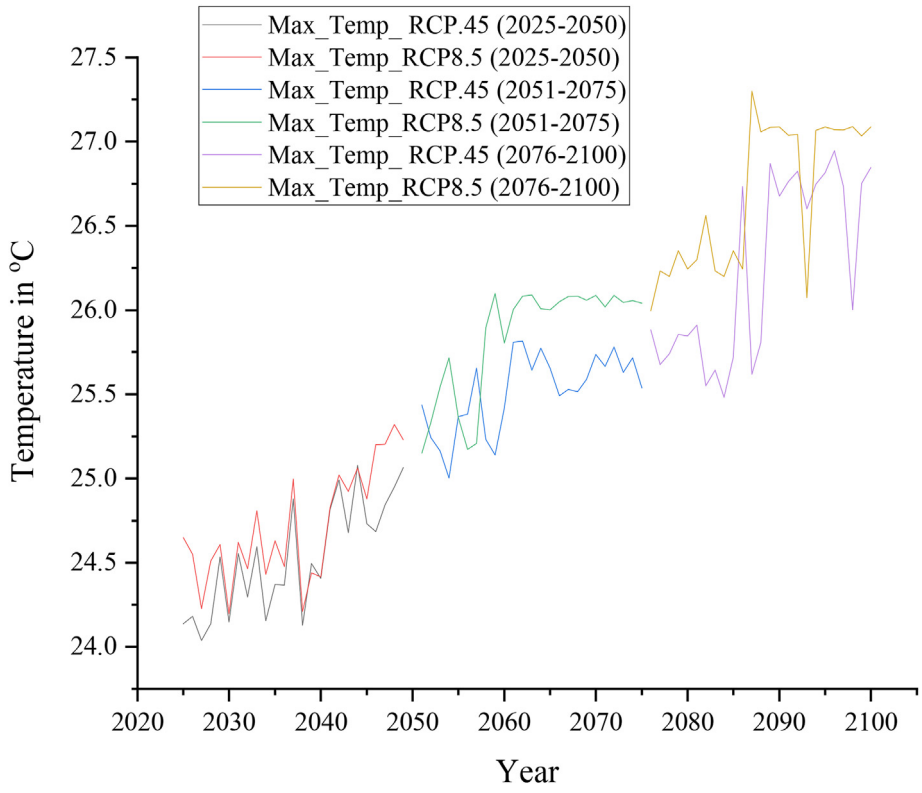

Figure 5. Projected change in annual maximum temperature under RCP4.5 and RCP8.5 emission scenarios during (2025–2100).

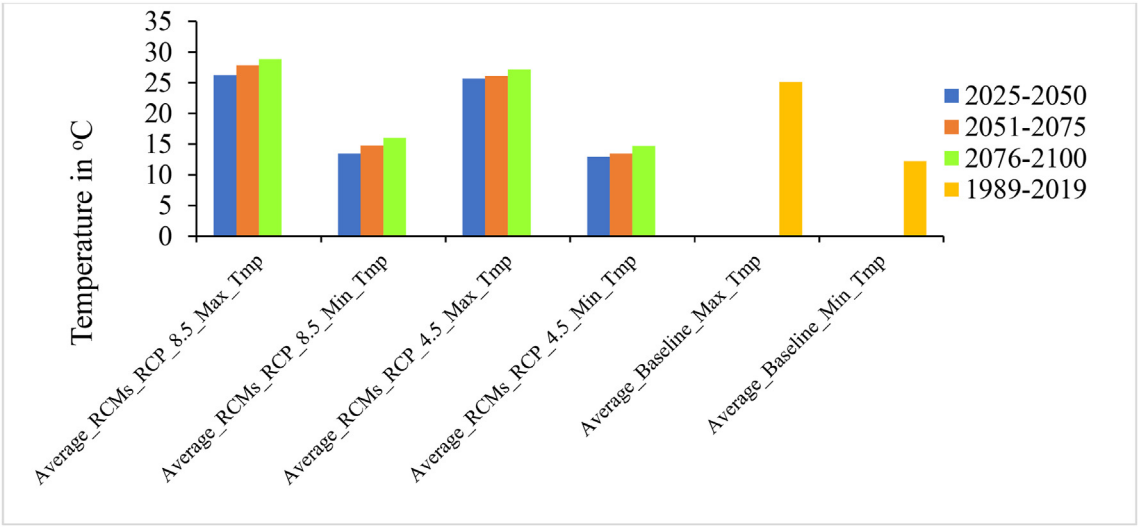

Figure 6. Changes in annual average maximum and minimum temperatures projected in the RCP 4.5 and RCP 8.5 emissions scenarios over the period (2025–2100) and observed over the period (1989–2019).

considered acceptable for the Omo-Gibe Great Abilite station and the SWAT model calibrated to capture the characteristics of the streamflow has similar trends as that of the observed streamflow (Table 4). The streamflow generated by SWAT for the reference period represents the actual streamflow data for the calibration and validation periods. Calibration and validation were conducted at a single location due to a lack of reliable upstream data. The model also predicted a decrease in streamflow in the basin, especially during the drier seasons and warmer than the rainy seasons, and simulated streamflow is well-represent precipitation. In general, the mean monthly hydrograph of observed versus simulated streamflow shows that the simulated and observed hydrographs have approximately identical patterns of calibration and validation (Figure 15) and (Figure 16).

5.4. Projected change in annual and seasonal streamflow

The future period (2025–2100) over 75-years simulated annual and seasonal streamflow change were evaluated and compared with the Baseline period (1991–2019) over 28-years The baseline period of fifteen streamflow gauging stations of the Omo-Gibe River Basin annual streamflow trend test change was analyzed. The baseline period of annual streamflow change and the data analyzed results showed a

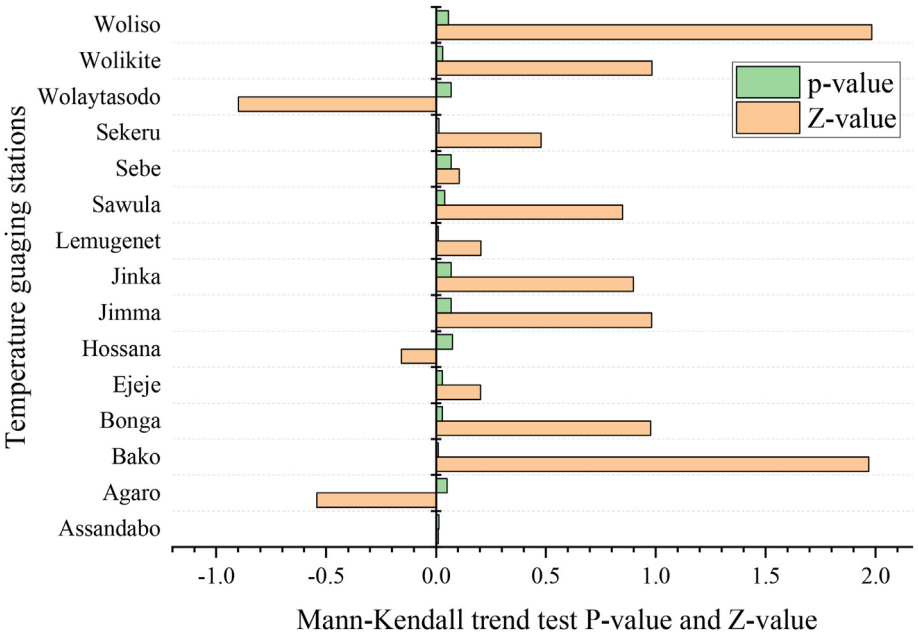

Figure 7. Changes in seasonal average temperature in Omo-Gibe River Basin during (1989–2019).

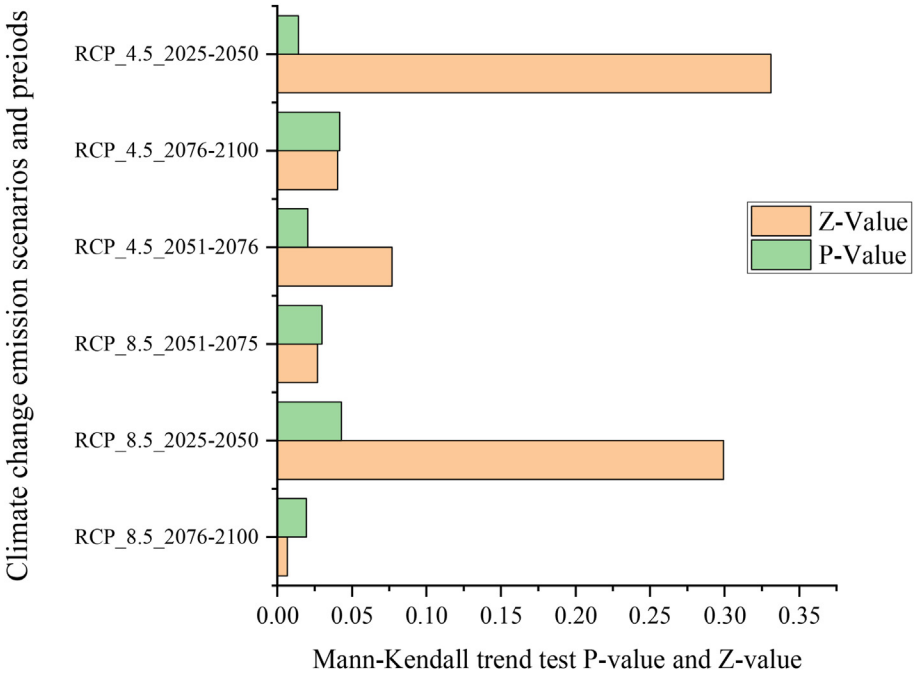

Figure 8. Change in projected average seasonal temperature under RCP 4.5 and RCP 8.5 emission scenarios over the period (2025–2100).

statistically significant decreasing trend (Figure 17), along with the projected annual streamflow under the RCP 4.5 and RCP 8.5 emissions scenarios, the analyzed results showed a significant downward trend (Figure 18). On the other hand, the trend test analyzed result found that the seasonal streamflow simulated and predicted under the RCP 4.5 and RCP 8.5 emissions scenarios declined trend in the future period (Figure 19).

In three future periods, the estimated and predicted seasonal and annual streamflow magnitude were adjusted and evaluated in various ways. Streamflow magnitude annual total streamflow, dry season mean monthly streamflow, and rainy season monthly means streamflow projected and percentage change predicted and adjusted were compared to the baseline period. For all future three study periods, projected under RCP4.5 and RCP8.5 emission scenarios, the estimated and predicted future annual and seasonal streamflow magnitude will decrease compared to the reference era in the Omo-Gibe River Basin summarized in (Table 5).

6. Discussions

6.1. Implications of the impacts of climate change on the future evolution of trend changes in hydroclimatic variables

In the context of changing climate and increasing water shortage, water consumption, and demand, it is essential to analyze trends in annual precipitation, seasonal distribution, and river streamflow

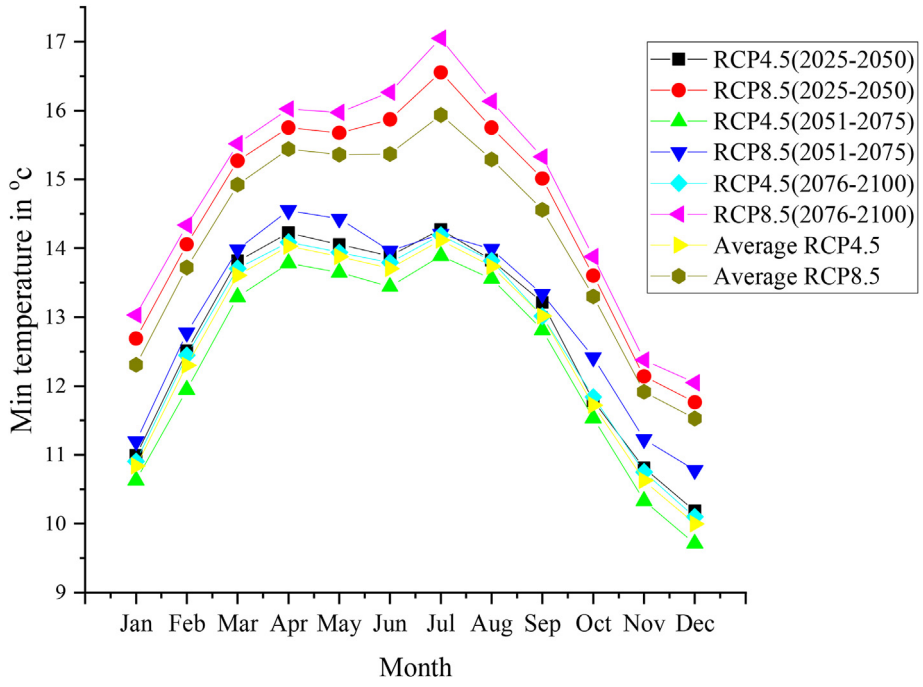

Figure 9. Projected monthly minimum temperature change under RCP 4.5 and RCP 8.5 emission scenarios over (2017–2100).

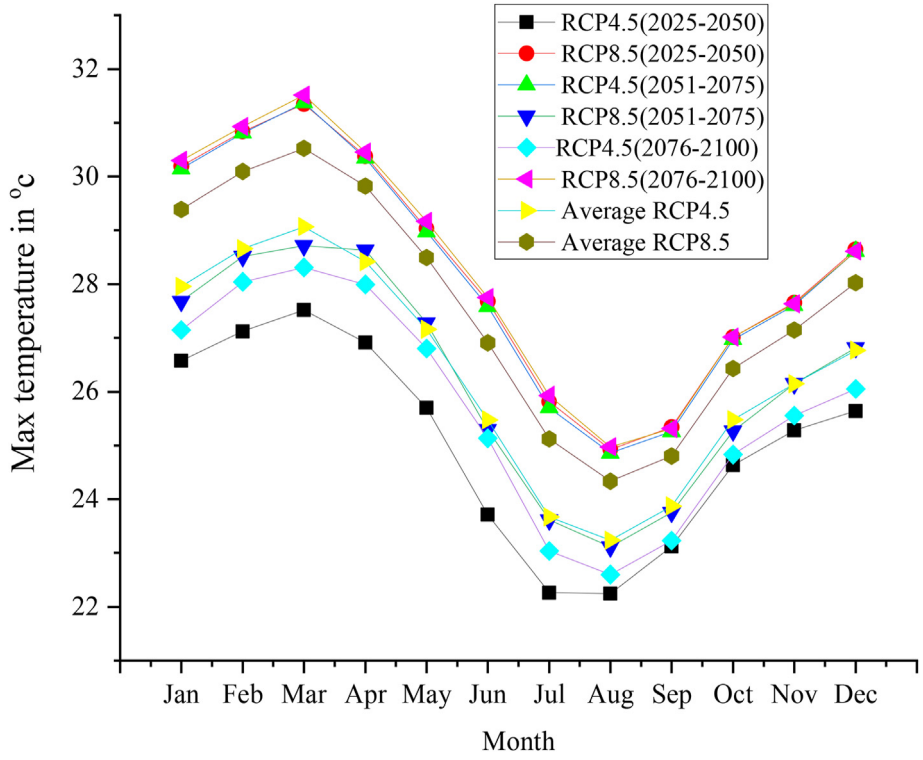

Figure 10. Projected monthly maximum temperature change under RCP 4.5 and RCP 8.5 emission scenarios over (2017–2100).

magnitude, as well as to assess the effects of these trends on the hydrological regime. In this section, observed and anticipated temperature rates, amount of precipitation, and magnitude of streamflow were assessed the statistical significance of the change and trend change using the non-parametric method of the MK test. Analyzing changes in trends in past, current, and future hydro-meteorological data can give us information and an idea of what to expect, as well as how to manage climate change impact, available water resources, and future water availability. This study evaluated the trend test of the hydroclimatic variables observed over the reference period (1989–2019) temperature, precipitation, and streamflow, and temperature, precipitation, and streamflow predicted according to the RCP4.5 and RCP 8.5 emission scenarios in three future periods (2025–2100) based on an annual and seasonal basis.

The basin as shown in (Figure 3), the observed mean annual air temperature, and (Figure 7) the seasonal air temperature results indicate

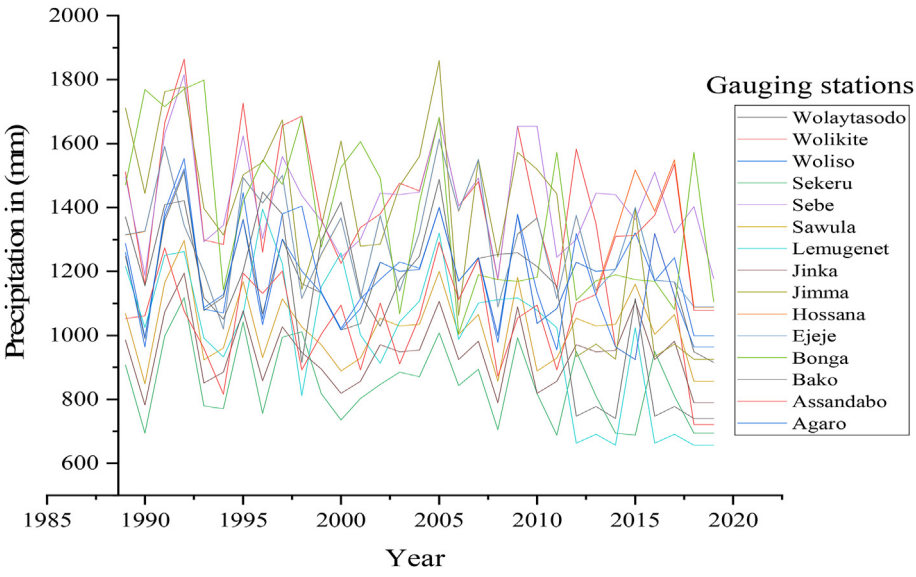

Figure 11. Observed annual precipitation changes in Omo-Gibe River Basin over the period (1989–2019).

Table 2. Annual and seasonal precipitation projected and percentage change.

Years	Baseline and projected total annual precipitation in (mm)	Projected change average annual precipitation in (mm)	Projected change average precipitation during the main rainy season in (mm)	Percentage change projected average precipitation in the main rainy season (%)	Projected change average precipitation during the erratic rainy season in (mm)	Percentage change projected average precipitation in the erratic rainy season (%)
PR_ Baseline period 1989–2019	14400.70	-	-	-	-	-
Pr_RCP_85_ 2025–2050	13058.04	1088.17	614.19	10.13	473.99	12.08
Pr_RCP_85_ 2051–2075	12017.30	1001.44	612.49	11.17	388.95	13.98
Pr_RCP_85_ 2076-2100	10791.60	982.63	603.08	13.18	379.55	14.54
Pr_RCP_45_ 2025–2050	13060.08	1090.01	614.27	10.12	475.74	11.42
Pr_RCP_45_ 2051–2075	12089.50	1007.46	615.50	11.17	391.96	12.79
Pr_RCP_45_ 2076-2100	11869.03	999.09	606.31	12.72	392.78	13.55

generally a strong statistically significant increasing trend (1989–2019). The temperature of the nine meteorological stations' time-series data in the reference period showed a significant level (0.05) upward trend at the eleven meteorological gauging stations, while two meteorological gauging station time-series data results showed a significant upward trend, as well as two stations, found no statistically significant monotonic trend change.

In the basin, as shown as illustrated in (Figure 6), the projected mean annual air temperature, and (Figure 8) the projected mean seasonal air temperature is generally shown a strong statistically significant increasing trend. Projected annual minimum and maximum temperatures under RCP4.5 and RCP8.5 emission scenarios trend tests results indicated strong increasing trends at the significance level (0.05) in the three future study periods (Figure 4 and Figure 5) respectively. Similarly projected average seasonal temperature under RCP4.5 and RCP 8.5 emission scenarios trend test results indicated strong increasing trends at the significance level (0.05) in the three future study periods (Figure 6). Projected annual and seasonal temperatures are generally shown a increasing trend for three-time windows near the future (2025–2050), middle future (2051–2075), and far future (2076–2100). Similarly, earlier research has found that the expected temperature increases under RCP4.5 and RCP 8.5 emissions scenarios agree with the findings of this study. A prior study in the Omo Gibe suggested that future temperatures might rise Chaemiso et al. (2016). Another study in Ethiopia's Awash River Basin Taye et al. (2018), as well as studies in the Ethiopian Central Rift Valley, Ziway River Basin Abraham et al. (2018), Upper Blue Basin Nile Basin Worku et al. (2021), all produced similar results.

Historical period, the time series precipitation data from the nine weather stations the test result showed a decreasing trend, whereas the precipitation data from the six weather stations showed no statistically significant monotonic decreasing or increasing trend. Annual precipitation (Figure 11) and seasonal precipitation (Figure 13) historical time series precipitation data showed an overall declining trend from (1989–2019).

Annual precipitation projected based on RCP 4.5 and RCP 8.5 emissions scenarios analyzed result showed a decreasing trend (Figure 12) while precipitation projected based on RCP 4.5 and RCP 8.5 emissions scenarios during the main summer rainy season and the spring rainy season trend test results showed a statistically significant level negative downward trend in three future periods see in (Figure 14). The annual and seasonal precipitation projected are generally shown a decreasing

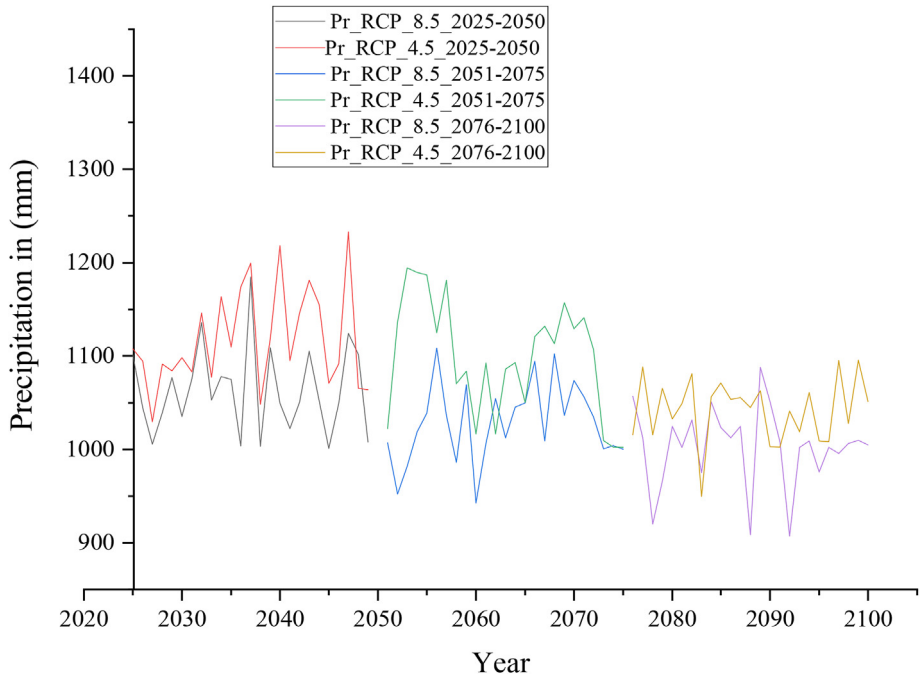

Figure 12. Projected annual precipitation change under RCP 8.5 and RCP 4.5 emission scenarios over (2025–2100).

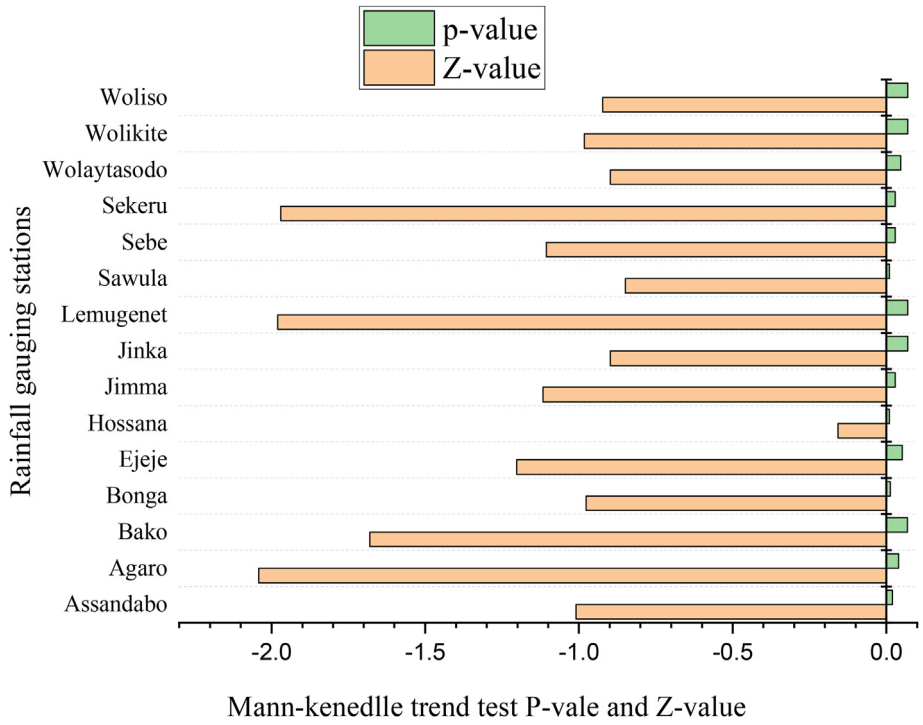

Figure 13. Observed seasonal precipitation change in Omo-Gibe River Basin over the period (1989–2019).

trend for three-time windows near future (2025–2050), middle future (2051–2075), and far future (2076–2100) a decreasing trend.

Historical annual streamflow changes were assessed from 1989 to 2019. In yearly streamflow models and forecasts, Figure 17 demonstrates a statistically significant (at the 0.05 level) downward trend (streamflow evaluation findings). Figure 18 depicts an estimated and projected yearly streamflow under the RCP 4.5 and RCP 8.5 emissions scenarios decreasing trend, whereas Figure 19 depicts an estimated and projected seasonal streamflow under the RCP 4.5 and RCP 8.5 emissions scenarios decreasing trend during (2025–2100). The historical period and the projected for the next three future periods streamflow showed a declining trend.

Overall, the trend test results demonstrated that the basin has a statistically significant trend of increasing temperature and a statistically significant trend of decreasing precipitation and streamflow over the three research periods. This is because climate change will have an impact on the future evolution of the trend change in the hydroclimatic variables of the river basin. It is expected to have an effect on the

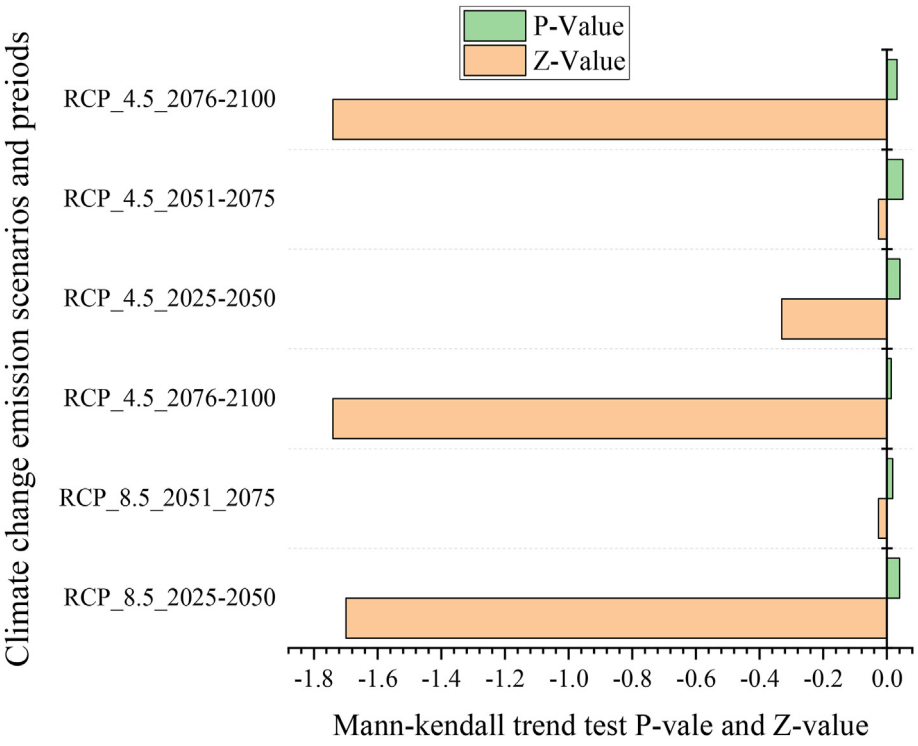

Figure 14. Projected seasonal precipitation change under RCP_4.5 and RCP_8.5 emission scenarios during (2025–2100).

Table 3. Streamflow parameters description names, fitted value, and allowable range, for calibration and uncertainty analysis.

Streamflow parameters change method, description, and names	Fitted Value	Allowable range
1: R_ SCS runoff curve number (CN2.mgt)	86.265	35–98
2: V_ Base flow alpha factor (ALPHA_BF.gw)	0.912	0–1
3: V_ Groundwater delay (GW_DELAY.gw)	412.941	30–450
4: R_ Maximum canopy storage (CANMX.hru)	0.294	0–10
5: V_ threshold depth of water in the shallow aquifer (GWQMN.gw)	3186.274	0–5000
6: R_ Groundwater "revap" coefficient (REVAPMN.gw)	132.353	0–500
7: R_ Depth from the soil surface to bottom of layer (SOL_Z.sol)	1441.176	0–3000
8: R_ saturated hydraulic conductivity (SOL_K(..).sol)	44.118	0–100
9: R_ Available water capacity of the soil layer (SOL_AWC(..).sol)	0.284	0–1
10: R_ soil evaporation compensation factor (ESCO.hru)	0.382	0–1
11: R_Effective hydraulic conductivity in main channel alluvium (CH_K2.rte)	0.735	0–1
12: R_ Groundwater "revap" coefficient (GW_REVAP.gw)	0.089	0.02–0.2
13: R_ Manning's "n" value for the main channel (CH_N2.rte)	0.618	0–1
14: R_ Plant uptake compensation factor (EPCO.hru)	0.598	0–1
15: R_ Initial depth of water in the deep aquifer (DEEPST.gw)	29901.961	0–50000
16: R_ Initial groundwater height (GWHT.gw)	11.520	0–25
17: R_ Fraction of porosity anions are removed ANION_EXCL.sol	0.382	0–1
18: R_ Deep aquifer percolation fraction (RCHRG_DP.gw)	0.637	0–1
19: R_ Saturated hydraulic conductivity (SOL_ZMX.sol)	583.333	0–3500

V_ means the existing parameter value is to be replaced by a given value and R_ means an existing parameter value is multiplied by (1+ a given value) Source: Neitsch et al. (2011).

reservoir's future water supply for hydroelectricity, irrigation, rain-fed agriculture, and other uses.

6.2. Impacts of climate change on the annual and seasonal temperature

This section focuses on predicting and estimating rates of temperature change resulting from future impacts of climate change. This is based on temperature projections change from CORDEX Africa's high-resolution regional climate model output data. All individual averages and 15 averages of the bias-adjusted temperature output showed a higher predicted temperature change than the reference period shown in (Figure 4, Figure 5, and Figure 6). The annual mean, maximum and minimum temperatures for the reference period were 23.10, 12.10, and 25.20 °C respectively, as shown in the graph (Figure 3). The average minimum and maximum temperatures predicted for three future eras under RCP 4.5 and RCP 8.5 emissions scenarios show a unidirectional increase with varying rates of change (Figure 6) compared to the reference period every season, and all years (Figure 4 and Figure 5). Minimum and maximum temperatures predicted for three future eras under RCP 4.5 and RCP 8.5 emissions scenarios also show a unidirectional increase with varying rates of change (Figure 4 and Figure 5) respectively compared to the reference period. Similarly, the minimum and maximum temperatures predicted under RCP 4.5 and RCP 8.5 emissions scenarios increased, as seen in (Figures 9 and 10) in all future predictions, except for a difference in the degree of change. For all individual bias RCM output and the mean values across the entire model output, the projected temperature change is expected to be unidirectional in ascending order, with the highest increase occurring at (2076–2100), followed by (2051–2075) and (2025–2050) during the research periods.

Table 4. Statistical performance indicators of model calibration and validation.

Performance Rating	NSE	R^2	PBIAS	P-factor	R-factor
Calibration	0.87	0.86	4.2	0.34	0.25
Validation	0.86	0.85	3.3	0.29	0.15

Table 5. Predicted changes in annual and seasonal streamflow under RCP 4.5 and RCP 8.5 (2025–2100).

Years	Simulated total annual streamflow (m^3/s)	Monthly mean streamflow (m^3/s)	Annual mean streamflow percentage change %	Dry season mean monthly streamflow (m^3/s)	Dry season mean monthly streamflow percentage change %	Rainy season monthly mean streamflow (m^3/s)	Rainy season monthly mean streamflow percentage change %
Baseline_ 1991–2019	5142.6	428.56	-	204.26	-	224.3	-
RCP_85_ 2025–2050	4838.4	400.4	7.02	191.6	4.02	211.6	3.00
RCP_85_ 2051–2075	4802.4	390.6	8.78	190.1	4.54	210.1	3.23
RCP_85_ 2076-2100	4837.2	370.8	10.99	191.55	6.22	211.6	4.77
RCP_45_ 2025–2050	4940.4	410.7	10.98	195.85	6.52	215.9	4.46
RCP_45_ 2051–2075	4929.6	400.8	11.93	195.4	7.20	215.4	4.73
RCP_45_ 2076-2100	4903.2	380.6	12.88	194.3	8.00	214.3	4.88

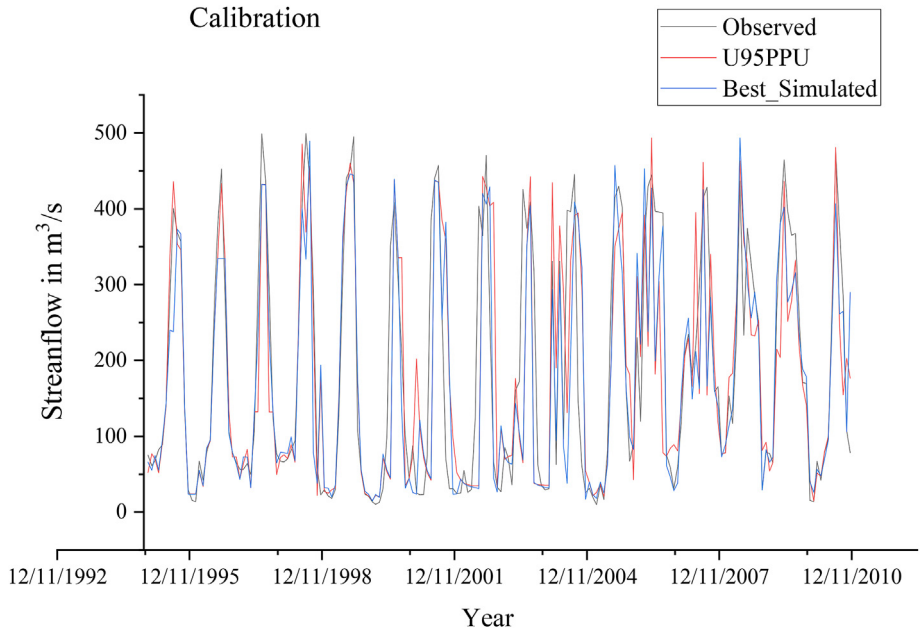

Figure 15. Hydrograph of the model calibration and uncertainty analysis monthly streamflow (1995–2010).

The projected annual average minimum temperature under RCP 4.5 emission scenarios increases the range between 1-2.69 °C while under RCP 8.5 emission scenarios increase the range between 2-3.56 °C shown as (Figure 6). Also, the projected change in annual average maximum temperature under RCP 4.5 emission scenarios increases the range between 2.40-3.36 °C while under RCP 8.5 emission scenarios increase the range between 2.6-4.56 °C shown as (Figure 6). Temperature change under RCP8.5 emission scenarios is larger and more severe than under RCP4.5 emission scenarios, according to this study. This indicates that RCP8.5 has the largest carbon emission scenario compared to RCP4.5. The findings of this investigation corroborated those of a prior study (IPCC, 2013). Other studies have confirmed that this study is in the medium RCP 4.5 and high RCP 8.5 emissions scenarios and that the anticipated temperature result for Africa is closely linked to the IPCC temperature predictions, showing a 2 °C increase in annual mean temperature by the middle of the twenty-first century, rising to 3–6 °C by the end of the century (Niang et al., 2014). Temperature increases of more than 2 °C in various Ethiopian areas were also confirmed in this investigation (Funk et al., 2008; Elshamy et al., 2008; Anyah et al. Qiu, 2012) and on future global and regional temperature rise (IPCC, 2014), the future temperature rises in Ethiopia (Ayalew, 2019), and future temperature increases in East Africa (Christensen et al., 2007; IPCC, 2013).

Projected changes in minimum and maximum temperatures seasonal (Figure 8) and monthly (Figure 9 and Figure 8) under RCP 4.5 and RCP 8.5 emission scenarios were assessed during the three study periods temperature is expected to increase in the future. The temperature is expected to increase from November to May, while it is projected to decrease from June to October, relative to other months in the river basin. Temperatures are higher during the hot dry season, while they are lower during the rainy season. The projected temperature from January to May is higher than in the other months of the year. This predicted temperature rise will impact future precipitation, streamflow, and water availability in the river basin. The increase in temperatures, according to Piani et al. (2010), can lead to a decrease in precipitation in certain areas, which is related to the length of the seasonal distribution and the amount of precipitation, as well as the frequency of catastrophic droughts. High temperatures can improve the ability to increase evapotranspiration, lower soil moisture content, increase the number of hot days per year by

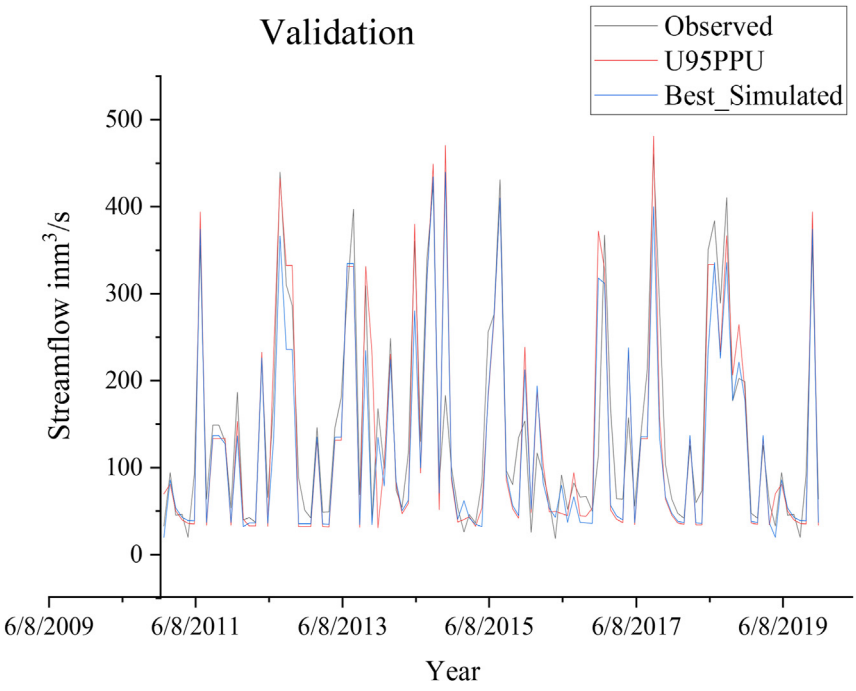

Figure 16. Hydrograph of the model validation and comparisons of observed and simulated monthly streamflow (2011–2019).

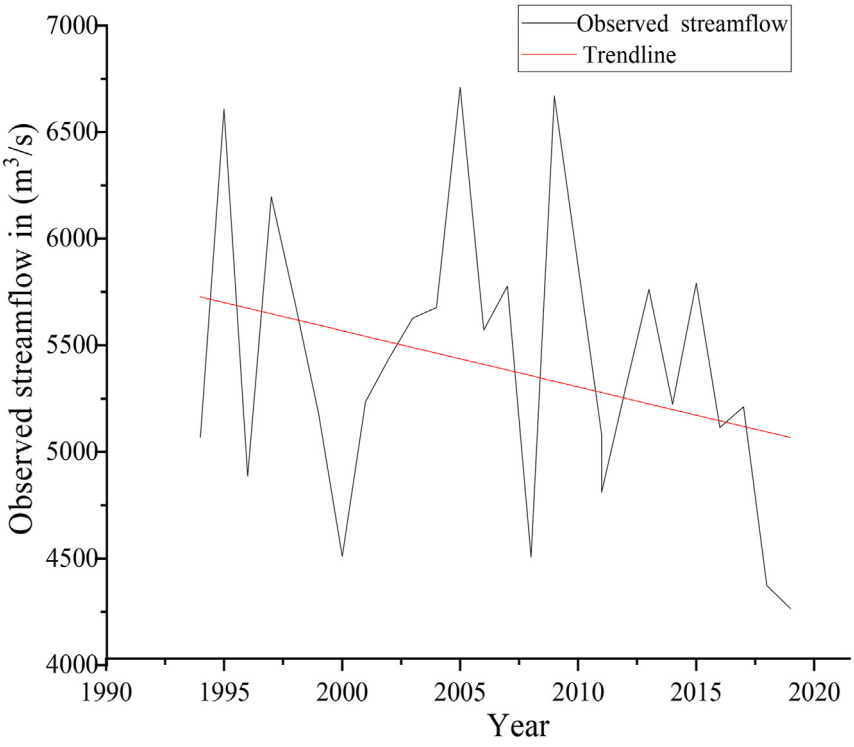

Figure 17. Historical annual streamflow change in the baseline period during (1991–2019).

lowering the number of cold days and reduce water throughput and availability. This means that for the same quantity of precipitation, less rain will reach river streams, reducing streamflow. Fluctuations and temperature rises, as well as variations and decreases in precipitation, will have an impact on water availability. This is partly because as temperatures rise, larger evaporation rates are predicted. In the future, the Omo gibe River Basin is predicted to see higher temperatures and more water stress.

6.3. Impacts of climate change on the annual and seasonal precipitation

Precipitation is the most important climate variable since it influences streamflow and water availability in the river basin in both direct and indirect ways. This section focuses on precipitation estimates and projections as a result of future climate change impacts, as well as changes in distribution. Three future period results indicated lower than the observed baseline period under RCP 4.5 and RCP 8.5 emission scenarios

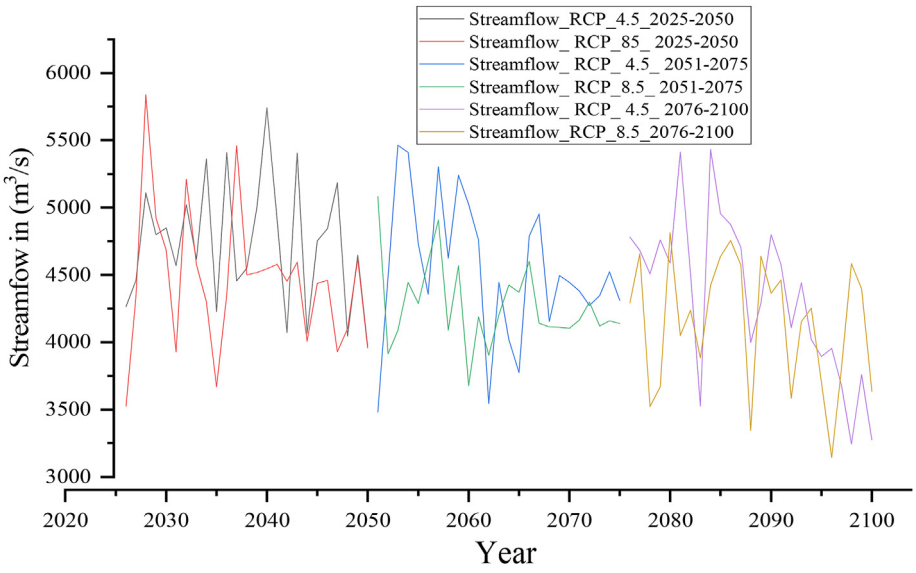

Figure 18. Changes in predicted annual streamflow under RCP 4.5 and RCP 8.5 emission scenarios over (2025–2100).

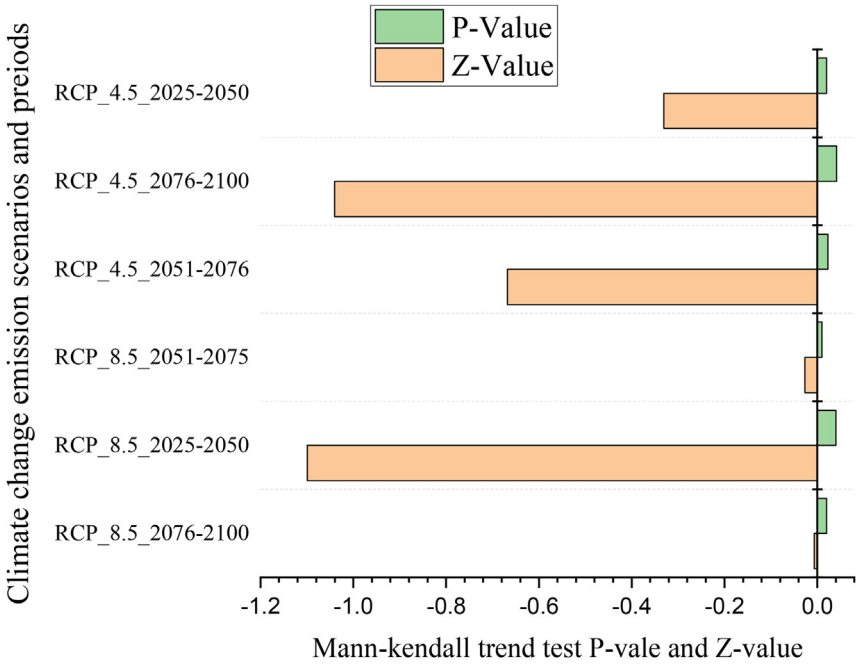

Figure 19. Change in predicted seasonal streamflow under RCP_4.5 and RCP_8.5 emission scenarios during (2025–2100).

predicted annual amount precipitation in (mm) (Table 2 and Figure 12) and seasonal precipitation distribution (Table 2). In comparison to reference periods, the projected precipitation distribution for the two rainy seasons, summer June to August, and Spring March to May, will decrease in the future (Table 2).

The annual total and average annual precipitation of the river basin were assessed to be 14,400.70 mm and 1,200.05 mm, respectively, at the current count of the reference period (2089–2019) (Table 2). In three future periods near future (2025–2050), the middle future (2051–2075), and the far future (2076–2100), the total annual precipitation, the annual averages, and the precipitation during the summer rainy season and the erratic spring season projected under RCP 4.5 and RCP 8.5 emissions scenarios will decrease compared to the reference period shown in (Table 2 and Figure 12). All individual bias-corrected RCMs had nearly identical degrees of decrease in predicted precipitation amount and seasonal distribution. During the summer main rainy season, from June to August, and the spring erratic rainy season, from March to May, the mean monthly precipitation distribution for most of the individual RCM values decreases, indicating one direction in decreasing order. Projected annual precipitation declines greatest over the period (2076–2100), followed by (2051–2075) and (2025–2050).

Over the study periods, the average annual precipitation expected to change under the RCP 4.5 emission scenarios decreases between 10.77 and 13.11% while the RCP 8.5 emission scenarios decrease between 11.10-13.86 %. The expected decrease in precipitation under the RCP 4.5 climate change scenario is less than the expected decrease in precipitation under the RCP 8.5 emissions scenario. Predicted monthly average precipitation change during the summer main rainy season and irregular rainy season decreases range 10.12–12.7 % and 11.42–13.55% under the RCP 4.5 emission scenarios while 10.13–13.18 % and 12.08–14.54 under

the RCP 8.5 emission scenarios respectively. However, the projected decrease in annual precipitation under PCR 8.5 is the largest in the window (2075–2100) relative to the two study windows (2051–2075) and (2025–2050). The major rainy season in the Omo-Gibe River basin runs from June to August, with an irregular rainy season from March to May. Declines in the irregular rainy season from March to May are higher than during the main rainy season from June to August, during study periods, and under the two emission scenarios.

The findings of this study confirmed those of previous studies. For example, a study conducted between 2000 and 2100 that used four IPCC emission scenarios (A1FI, A2, B1, and B2) and five GCMs (HadCM3, PCM, CGCM2, CSIRO2, and ECHAM4) found that rainfall in the Horn of Africa (including Ethiopia) might decrease by 25% (Faramarzi et al., 2013). Globally and regionally, climate change adversely affects the amount and distribution of annual and seasonal precipitation (Giorgi et al., 2011). According to another study, as a result of climate change, precipitation, pattern amount, and distribution will change and decrease (Osima et al., 2018; IPCC, 2014). Other research has revealed similar fund outcomes as a result of projected precipitation decreases due to climate change (Peleg et al., 2014; Samuels et al., 2018). Significant change and decrease in precipitation resulting in climate change, which corresponds to the IPCC estimate for Eastern Africa at the end of the 21st century (Christensen et al., 2007; IPCC, 2013).

The main rainy season in the Omo-Gibe River Basin is between June and August in summer and March and May in spring. These are the most important rainy seasons in the watershed, which affect future annual precipitation and seasonal distribution, and also act as a major contributor to precipitation and the hydrological driver. The magnitude of future streamflow will be influenced by the amount of precipitation that is expected to reduce seasonal streamflow in the future. It is also the major input to the river basin streamflow magnitude. The expansion of irrigation has occurred in the basin due to the creation of large irrigation projects in the lower Omo valley and three existing dams, the center under construction of the fourth dam and the fifth dam planned for the basin of Omo-gibe. Thus, during these months, the decrease in precipitation combined with the increase in temperature will impact the streamflow of the basin, the available water, the production of hydropower production, the practices of irrigation, agricultural production, community livelihoods rain-fed agriculture, drinking water, livestock water, and pasture for the lowland nomadic populations of the basin.

6.4. Impacts of climate change on future annual and seasonal streamflow

Impacts of climate change on future annual and seasonal streamflow assessed results are presented in this section. ssess and predict changes in streamflow magnitude due to the future impacts of climate change. Assessed and predicted total annual, annual mean, seasonal mean, and monthly mean streamflow under RCP4.5 and RCP8.5 emissions scenarios showed a significant reduction in the future for all study periods compared to the reference period (Table 5 and Figure 18). At the end of the 21 century, the annual and seasonal streamflow of the river basin is projected to be the lowest (2076–2100) compare to two windows (2025–2050) and (2051–2075). This decrease in annual and seasonal streamflow in the Omo-gibe Basin is linked to increased temperature, decreased precipitation, and decreased streamflow during rainy, hot, and dry seasons during three future research periods, relative to the baseline period.

According to the PCR 4.5 emission scenarios predicted the highest monthly average streamflow decrease by 410.7 m^3/s, 400.8 m^3/s, and 380.6 m^3/s near future (2025–2050), middle future (2051–2075), and far future (2075–2100) respectively, while under 8.5 scenarios the highest monthly average streamflow decreases to be 400.4 m^3/s, 390.6 m^3/s, and 370.8 m^3/s compare to reference period see (Table 5) respectively. Predicted annual average streamflow change during the driest autumn (September–November) and the hottest winter (December–February rainy summer season (June–August) and the irregular rain season (March–May) decrease range 7.08–10.99% under the RCP 4.5 emission scenarios, while under the RCP 8.5 emission scenarios decrease range 10.98–12.88%. Predicted monthly average streamflow change during the driest autumn (September–November) and the hottest winter (December–February) decrease range 4.02–6.22% under the RCP 4.5 scenario and 6.52–8.00% under the RCP 8.5 emission scenarios shown in (Table 5). Predicted monthly average streamflow change during the summer rainy season and irregular rainy season decreases range from 3.00-4.77 % under the RCP 4.5 emission scenarios while 4.46–4.88 % under the RCP 8.5 emission scenarios shown in (Tabel 5). The estimated and predicted seasonal streamflow likely follows the predicted precipitation pattern; it is expected to decrease and change two rainy seasons and the driest and the hottest seasons.

The results of this study revealed that the streamflow in the river basin will decrease in the future. The previous studies are supports this study's results according to (Kabobah et al., 2016), streamflow will change and decrease in the future due to climate change and its dependence on rainfall. Another study similarity suggests that future decreases in streamflow will be linked to projected decreases in precipitation (Saeed et al., 2022), as confirmed by this study's results. The change and decrease in streamflow shown by this study in the RCP 4.5 and RCP 8.5 global emissions scenarios are consistent with previous research (Amisigo et al., 2015). Similarly, Bessah et al. (2020) found that future impacts of climate change may lead to a decrease in mean annual streamflow. The results of this study are also consistent with other studies showing an expected decrease in streamflow due to climate change (Dao Nguyen and Suetsugi, 2012; IPCC, 2014; Xuan Hoan, 2020). Another study in Ethiopia found that the streamflow will decrease in the future (Ayalew 2019). Rainy seasons are projected to have significant reductions in streamflow in the future under both RCP 4.5 and RCP 8.5 climate emissions scenarios (Shrestha et al., 2018; Kim and Choi, 2013), and this study found it confirmed.

The above research results show that streamflow will be affected by the joint actions of increasing temperature and decreasing precipitation. According to the findings of this study, streamflow is highly sensitive to temperature and precipitation. These findings are consistent with the findings of this study (Saha and Zeleke, 2015). Moreover, the research results show that precipitation, temperature, and streamflow all have a close relationship. The reduction in predicted streamflow magnitude during the summer rainy season is less than that during the erratic rainy season. The increase in temperature and the decrease in precipitation during the two rainy seasons will have an impact on the streamflow of the basin. The decrease in the magnitude of the seasonal streamflow is greater in the two future hot and dry seasons than in the two rainy seasons. The annual and two rainy seasons' precipitation has a greater influence on the magnitude of the annual and seasonal streamflow than in the hot, and dry seasons. According to two scenarios RCP 4.5 and RCP 8.5, the reduction in the projected streamflow during the three research periods is significant for both the wet, hot and dry seasons. The main causes of significant changes in river streamflow are changes in precipitation amounts and patterns. In the future, this could lead to a reduction in the amount of water available for various uses in the river basin.

7. Conclusions

This study predicted the potential impacts of climate change on future precipitation amounts, seasonal distribution, and streamflow in the Omo-Gibe River basin. Climate change conditions in the basin were projected using high-resolution regional climate models CORDEX-Africa for two emission scenarios RCP 4.5 and RCP 8.5 for three-time windows near future (2025–2050), middle future (2051–2075), and far future (2076–2100) compared a project with the reference period (1989–2019). The Mann-Kendall trend test was used to determine whether a change is statistically significant and to detect trends of the baseline line period and future periods of projected temperature,

precipitation, and streamflow. The Soil and Water Assessment Tool (SWAT) hydrology model was used to predict the impact of climate change on future streamflow magnitude.

Over the three research periods, the estimated and expected annual, seasonal, and monthly temperature changes increase significantly and the expected annual, seasonal, and monthly precipitation and streamflow decrease significantly. Annual and seasonal temperature predictions under RCP 4.5 and RCP 8.5 show a statistically significant upward trend. Although annual and seasonal precipitation and streamflow predictions under PCR 4.5 and PCR 8.5 show a statistically significant negative declining trend.

Overall, the projected average temperature increase is 2.40–3.34 °C under RCP 4.5 emission scenarios, while 2.6–4.54 °C under RCP 8.5. The projected average annual precipitation decrease range is 10.77–13.11 % in the RCP 4.5 emission scenarios whereas the RCP 8.5 emission scenarios decrease range is 11.10–13.86% %. The projected streamflow decrease range is 7.08–10.99 % under the RCP 4.5 scenario while the RCP 8.5 emission scenarios change decrease range is 10.98–12.88%. Compared to the reference period, the PCR 8.5 emissions scenarios show significant changes in temperature, precipitation, and streamflow compared to the PCR 4.5 emissions scenarios over three study periods. Streamflow responds linearly to variations in precipitation and temperature. On the other hand, the direction of expected precipitation and temperature changes have a significant effect on expected streamflow changes.

In the Omo-Gibe River basin in the future, there will be significant annual, seasonal, and monthly increases in temperature and decreases in precipitation and streamflow. Projected precipitation decreases, while temperatures increase, resulting in a decrease in streamflow. There was a statistically significant relationship between streamflow, precipitation, and temperature. In addition, the results showed a strong link between increased temperatures and decreased precipitation and streamflow, showing a significant relationship between the two factors that will reduce future water availability in the river basin. The findings of the study highlight the importance of establishing sustainable water management in the future to reduce the impacts of climate change. Land-use changes, on the other hand, were not included in this study. As things are likely to change in the future, there will be more uncertainty. Changes in the basin are expected, including an increase in temperature rates, a decrease in the amount and distribution of precipitation, and a decrease in the magnitude of streamflow. Finally, we suggest implementing feasible and appropriate adaptation and mitigation techniques and measures as early as possible to minimize future impacts of climate change in this basin. Future water availability for hydroelectric power generation, irrigation, rain-fed agriculture, and other sectors could be impacted if appropriate adaptation and mitigation measures are not implemented in the basin.

Declaration

Author contribution statement

Tamiru Paulos: Conceived and designed the experiments; Performed the experiments; Analyzed and interpreted the data; Wrote the paper.

Gordana Kranjac-Berisavijevic & Felix K. Abagale: Conceived and designed the experiments; Contributed reagents and interpreted the data.

Funding statement

This work was supported by the West African Centre for Water, Irrigation and Sustainable Agriculture (WACWISA), University for Development Studies, Ghana and the Government of Ghana and World Bank through the African Centres of Excellence for Development Impact (ACE Impact) initiative.

Data availability statement

The data that has been used is confidential. Most of the data used in this research article are received from (https://glovis.usgs.gov/app), NMAE (National Meteorology Agency of Ethiopia) (https://pcmdi.llnl.gov/mips/cmip5/data-portal.html) WIEE (Water, Irrigation, and Electricity of Ethiopia).

Declaration of interest's statement

The authors declare the following conflict of interests:

1. Mr. Tamiru Paulos Orkodjo

Affiliation:- Department of Agricultural Engineering, School of Engineering, University for Development Studies, Tamale-Ghana

2. Professor. Gordana Kranjac-Berisavijevic

Affiliation:- Department of Agricultural Mechanisation & Irrigation Technology Faculty of Agriculture and Consumer Sciences, UDS, PO Box 1882, Nyankpala

3. Professor. Felix K. Abagale

Affiliation: Department of Environment, Water and Waste Engineering, School of Engineering, University for Development Studies, Tamale-Ghana

Additional information

No additional information is available for this paper.

References

Abatzoglou, J.T., Brown, T.J., 2012. A comparison of statistical downscaling methods suited for wildfire applications. Int. J. Climatol. 32, 772–780, 2012.

AbbAspour, K.C., 2014. In: SWAT-CUP., 2012. SWAT Calibration and Uncertainty Programs – A User Manual. Swiss Federal Institute of Aquatic Science and Technology.

Abbaspour, K.C., SWAT-CUP., 2015. SWAT Calibration and Uncertainty Programs – A User Manual. Department of Systems Analysis, Integrated Assessment and Modelling (SIAM), Eawag. Swiss Federal Institute of Aquatic Science and Technology, Duebendorf, Switzerland, p. 100.

Abbaspour, M., Nazaridoust, A., 2007. Determination of environmental water requirements of Lake Urmia, Iran: an ecological approach. Int. J. Environ. Stud. 64 (2), 161–169.

Abraham, T., Woldemicheala, A., Muluneha, A., Abateb, B., 2018. Hydrological responses of climate change on lake Ziway catchment, Central Rift valley of Ethiopia. J. Earth Sci. Climatic Change 9 (474), 2.

Acharya, N., Chattopadhyay, S., Mohanty, U.C., Dash, S.K., Sahoo, L.N., 2013. On the bias correction of general circulation model output for Indian summer monsoon. Meteorol. Appl. 20 (3), 349–356.

Ahmad, I., Tang, D., Wang, T., Wang, M., Wagan, B., 2015. Precipitation trends over time using Mann-Kendall and Spearman's rho tests in Swat River Basin, Pakistan. Adv. Meteorol. 2015, 1–15.

Amirabadizadeh, M., Huang, Y.F., Lee, T.S., 2015. Recent trends in temperature and precipitation in the Langat river basin, Malaysia. Adv. Meteorol. 2015, 16. Article ID 579437.

Amisigo, Barnabas A., McCluskey, Alyssa, Swanson, Richard, 2015. Modeling impact of climate change on water resources and agriculture demand in the Volta Basin and other basin systems in Ghana. Sustainability 7 (6), 6957–6975.

Anandhi, A., Srinivas, V.V., Nanjundiah, R.S., Kumar, N.D., 2008. Downscaling precipitation to river basin in India for IPCC SRES scenarios using Support Vector Machine. Int. J. Climatol. 28, 401–420.

Angelina, A., Gado Djibo, A., Seidou, O., Seidou Sanda, I., Sittichok, K., 2015. Changes to flow regime on the Niger River at Koulikoro under a changing climate. Hydrol. Sci. J. 60 (10), 1709–1723.

Anghileri, D., Pianosi, F., Soncini-Sessa, R., 2014. Trend detection in seasonal data: fromhydrology to water resources. J. Hydrol. 511, 171–179.

Anyah, R.O., Qiu, W., 2012. Characteristic 20th and 21st century precipitation and temperature patterns and changes over the greater horn of Africa. Int. J. Climatol. 32, 347–363.

Arabi, M., Govindaraju, R.S., Hantush, M.M., 2007. A probabilistic approach for analysis of uncertainty in the evaluation of watershed management practices. J. Hydrol. 333, 459–471.

Arnell, N.W., Lowe, J.A., Brown, S., Gosling, S.N., Gottschalk, P., Hinkel, J., Lloyd-Hughes, B., Nicholls, R.J., Osborn, T.J., Osborne, T.M., Rose, G.A., Smith, P., Warren, R.F., 2013. A global assessment of the effects of climate policy on the impacts of climate change. Nat. Clim. Change 3, 512–519.

Arnold, J.G., Srinivasan, R., Muttiah, R.S., Williams, J.R., 1998. Large area hydrologic modeling and assessment- Part I: model development. J. Am. Water Resour. Assoc. 34 (1), 73–89.

Arnold, J.G., Moriasi, D.N., Gassman, P.W., Abbaspour, K.C., White, M.J., Srinivasan, R., Santhi, C., Harmel, R.D., van Griensven, A., van Liew, M.W., et al., 2012. SWAT: model use, calibration, and validation. Transact. ASABE 55 (4), 1345–1352.
Arnold, J.G., Moriasi, D., Gassman, P., Abbaspour, C.K., White, M., Srinivasan, R., Santhi, C., Harmel, D.R., van Griensven, A., Van Liew, M., Kannan, N., Jha, M., 2012a. SWAT: model use, calibration, and validation. Trans. ASABE (Am. Soc. Agric. Biol. Eng.) 55 (4), 1491–1508.
Arnold, J.G., Kiniry, J.R., Srinivasan, R., Williams, J.R., Haney, E.B., Neitsch, S.L., 2012b. Soil and Water Assessment Tool Input/Output File Documentation: Version 2012 (Texas Water Resources Institute TR-439). USDA-ARS, Grassland, Soil and Water Research Laboratory, and Texas AgriLife Research, Blackland Research and Extension Center, Temple, Texas.
Ayalew, D.W., 2019. Evaluating the Potential Impact of Climate Change on the Hydrology of Ribb Catchment. Master's thesis. Blue Nile Basin, Ethiopia.
Bae, D.H., Jung, I.W., Lettenmaier, D.P., 2011. Hydrologic uncertainties in climate change from IPCC AR4 GCM simulations of the Chungju Basin, Korea. J. Hydrol. 401, 90–105.
Bekele, D., Alamirew, T., Kebede, A., Zeleke, G., Melesse, M., A., 2018. Modeling climate change impact on the hydrology of keleta watershed in the Awash River basin, Ethiopia. Environ. Model. Assess.
Bessa Santos, R.M., Sanches Fernandes, L.F., Vitor Cortes, R.M., Leal Pacheco, F.A., 2019. Development of a hydrologic and water allocation model to assess water availability in the Sabor River Basin (Portugal). Int. J. Environ. Res. Publ. Health 16, 24190.
Bessah, E., Raji, A.O., Taiwo, O.J., Agodzo, S.K., Ololade, O.O., Strapasson, A., 2020. Hydrological responses to climate and land use changes: the paradox of regional and local climate effect in the Pra River Basin of Ghana. J. Hydrol.: Reg. Stud. 27, 100654.
Central Statistics Agency, 2017. Ethiopian National Population and Housing Census. Central Statistical Agency, Addis Ababa, 385 p.
Chaemiso, S.E., Abebe, A., Pingale, S.M., 2016. Assessment of the impact of climate change on surface hydrological processes using SWAT: a case study of Omo-Gibe river basin, Ethiopia. Modeling Earth Syst. Environ. 2 (4), 1–15.
Chien, H., Yeh, P.J.-F., Knouft, J.H., 2013. Modeling the potential impacts of climate change on streamflow in agricultural watersheds of the Midwestern United States. J. Hydrol. 491, 73–88.
Chow, V.T., 1964. Handbook of Applied Hydrology. McGraw-Hill Book Company, New York, NY, USA.
Christensen, J.H., Hewitson, B., Busuioc, A., Chen, A., Gao, X., Held, I., Jones, R., Kolli, R.K., Kwon, W.T., Laprise, R., Rueda, V.M., Mearns, L., Menéndez, C.G., Räisänen, J., Rinke, A., Sarr, A., Whetton, P., 2007. Regional Climate Projections, Climate Change 2007: the Physical Science Basis. Contribution of Working Group I to the Fourth Assessment Report of the Intergovernmental Panel on Climate Change. Cambridge University Press, Cambridge.
Dao Nguyen, Khoi, Suetsugi, Tadashi, 2012. Uncertainty in climate change impacts on streamflow in Be River Catchment. Vietnam Water Environ. J. 26 (4), 300–309.
Dao Nguyen, Khoi, Thom, Vu Thi, Xuan Quang, Chau Nguyen, Phi, Ho Long, 2017. Parameter uncertainty analysis for simulating streamflow in the upper Dong Nai river basin. La Houille Blanche 103 (1), 14–23.
Degefu, M.A., Bewket, W., 2014. Variability and trends in rainfall amount and extreme event indices in the Omo-Ghibe River Basin, Ethiopia. Reg. Environ. Change 14 (2), 799–810.
Dessu, S.B., Melesse, A.M., 2013. Impact and uncertainties of climate change on the hydrology of the Mara River basin, Kenya/Tanzania. Hydrol. Process. 27, 2973–2986.
Dominguez, F., Rivera, E., Lettenmaier, D.P., Castro, C.L., 2012. Changes in winter precipitation extremes for the western United States under a warmer climate as simulated by regional climate models. Geophys. Res. Lett. 39, 5.
Easterling, D.R., 1997. Maximum and minimum temperature trends for the globe. Science 277 (5324), 364–367, 1997.
Ebrahimian, M., Nuruddin, A.A., Soom, M.A.M., Sood, A.M., Neng, L.J., Galavi, H., 2018. Trend analysis of major hydroclimatic variables in the Langat River basin, Malaysia. Singapore J. Trop. Geogr. 39 (2), 192–214.
Ejder, T., Kale, S., Acar, S., Hisar, O., Mutlu, F., 2016. Restricted effects of climate change on annual streamflow of Sarıçay Stream (Çanakkale, Turkey). Marine Sci. Technol. Bull. 5, 7–11.
Elguindi, N., Grundstein, A., 2013. An integrated approach to assessing 21st-century climate change over the contiguous U.S. using the NARCCAP RCM output. Climatic Change 117, 809–827.
Elshamy, M.E., Seierstad, I.A., Sorteberg, A., 2008. Impacts of climate change on Blue Nile flows using bias-corrected GCM scenarios. Hydrol. Earth Syst. Sci. Discuss. 5 (3), 1407–1439.
Elsner, M.M., Cuo, L., Voisin, N., Deems, J.S., Hamle, A.F., Vano, J.A., Lettenmaier, D.P., 2010. Implications of 21st-century climate change for the hydrology of Washington State. Clim. Change 102 (1), 225–260.
Fabre, J., Ruelland, D., Dezetter, A., Grouillet, B., 2015. Simulating past changes in the balance between water demand and availability and assessing their main drivers at the river basin scale. Hydrol. Earth Syst. Sci. 19 (3), 1263–1285.
Fakult, M., Kiel, M.P.A., 2015. Guideline for Hydrologically Consistent Models. Published 2015. https://nbn.resolving.org/urn:nbn:de:gbv:8-diss-177500.
FAO, 2016. AQUASTAT website. Food and Agriculture Organization of the United Nations (FAO) [Online] Available at: http://www.fao.org/nr/water/aquastat/countries_regions/ETH/ [Revised 2016-04- 20].
Faramarzi, M., Abbaspour, K.C., Vaghefi, S.A., Farzaneh, M.R., Zehnder, A.J., Srinivasan, R., Yang, H., 2013. Modeling impacts of climate change on freshwater availability in Africa. J. Hydrol. 480, 85–101.
Ficklin, D.L., Stewart, I.T., Maurer, E.P., 2012. Effects of projected climate change on the hydrology in the Mono Lake Basin. California. Clim. Change 116, 111–131.
Friedlingstein, P., Houghton, R.A., Marland, G., Hackler, J., Boden, T.A., Conway, T.J., Canadell, J.G., Raupach, M.R., Ciais, P., Le Quéré, C., 2010. Update on CO2 emissions. Nat. Geosci. 3 (12), 811–812.
Fu, G., Charles, S.P., Yu, J., 2009. A critical overview of pan evaporation trends over the last 50 years. Climatic Change 97 (1-2), 193–214.
Funk, C., Dettinger, M.D., Michaelsen, J.C., Verdin, J.P., Brown, M.E., Barlow, M., Hoell, A., 2008. Warming of the Indian Ocean threatens eastern and southern African food security but could be mitigated by agricultural development. Proc. Natl. Acad. Sci. USA 105 (32), 11081–11086.
Gassman, P.W., Reyes, M.R., Green, C.H., Arnold, J.G., 2007. The soil and water assessment tool: historical development, applications, and future research directions. Transact. ASABE 50 (4), 1211–1250.
Gebrechorkos, S.H., Hülsmann, S., Bernhofer, C., 2019. Statistically downscaled climate dataset for East Africa. Sci. Data 6, 31.
Giorgi, F., Jones, C., Asrar, G., 2009. Addressing climate information needs at the regional level: the CORDEX framework. Organization (WMO) Bull 58 (July), 175–183.
Giorgi, F., Im, E.-S., Coppola, E., Diffenbaugh, N.S., Gao, X.J., Mariotti, L., Shi, Y., 2011. Higher hydroclimatic intensity with global warming. J. Clim. 24 (20), 5309–5324.
Green, W.H., Ampt, G.A., 1911. Studies on soil physics. J. Agric. Sci. 4 (1), 1–24.
Gupta, H.V., Sorooshian, S., Yapo, P.O., 1999. Status of automatic calibration for hydrologic models: comparison with multilevel expert calibration. J. Hydrol. Eng. 4 (2), 135–143.
Hamlet, A.F., Elsner, M.M., Mauger, G.S., et al., 2013. An overview of the Columbia Basin climate change scenarios project: approach, methods, and summary of key results. Atmos.-Ocean 51, 392–415.
Han, Z.Y., Tong, Y., Gao, X.J., 2018. Correction based on quantile mapping for temperature simulated by the RegCM4. Clim. Change Res. 14 (4), 331–340.
Hargreaves, G., Samani, Z.A., 1985. Reference crop evapotranspiration from temperature. Appl. Eng. Agric. 1, 96–99.
Hawkins, E., Osborne, T.M., Ho, C.K., Challinor, A.J., 2013. Calibration and bias correction of climate projections for crop modelling:an idealised case study over. Europe. Agric. For. Meteorol. 170, 19–31.
Hegerl, G.C., Zwiers, F.W., Braconnot, P., Gillett, N.P., Luo, Y., Marengo-Orsini, J.A., Nicholls, N., Penner, J.E., Stott, P.A., 2007. Understanding and attributing climate change. In: Solomon, S., et al. (Eds.), Climate Change 2007: the Physical Science Basis. Contribution of Working Group I to the Fourth Assessment Report of the Intergovernmental Panel on Climate Change. Cambridge Univ. Press, Cambridge, U. K, pp. 663–745.
Hijioka, K., Sonoda, K.H., Tsutsumi-Miyahara, C., Fujimoto, T., Oshima, Y., Taniguchi, M., Ishibashi, T., 2008. Investigation of the role of CD1d-restricted invariant NKT cells in experimental choroidal neovascularization. Biochem. Biophys. Res. Commun. 374 (1), 38–43.
Immerzeel, W.W., Van Beek, L., Konz, M., Shrestha, A., Bierkens, M., 2012. Hydrological response to climate change in a glacierized catchment in the Himalayas. Clim. Chang 110 (3–4), 721–736.
Intergovernmental Panel on Climate Change, 2012. In: Field, C.B., Barros, V., Stocker, T.F., Qin, D., Dokken, D.J., Ebi, K.L., Mastrandrea, M.D., Mach, K.J., Plattner, G.-K., Allen, S.K., Tignor, M., Midgley, P.M. (Eds.), Managing the Risks of Extreme Events and Disasters to Advance Climate Change Adaptation. A Special Report of Working Groups I and II of the Intergovernmental Panel on Climate Change. Cambridge University Press Cambridge, UK, and New York, NY, USA, p. 582.
Intergovernmental Panel on Climate Change, 2013. In: Stocker, T.F., Qin, D., Plattner, G.K., Tignor, M., Allen, S.K., Boschung, J., Nauels, A., Xia, Y., Bex, V., Midgley, P.M. (Eds.), Summary for Policymakers, Climate Change 2013: the Physical Science Basis. Contribution of Working Group I to the Fifth Assessment Report of the Intergovernmental Panel on Climate Change. Cambridge University Press, Cambridge, United Kingdom, and New York, NY, USA, p. 28.
Intergovernmental Panel on Climate Change IPCC, 2007. In: Solomon, S., et al. (Eds.), Climate Change 2007: the Physical Science Basis. Contribution of Working Group I to the Fourth Assessment Report of the Intergovernmental Panel on Climate Change. Cambridge Univ. Press, Cambridge, U. K, p. 996.
Intergovernmental Panel on Climate Change IPCC, 2014. Summary for policymakers. In: Field, C.B., Barros, V.R., Dokken, D.J., Mach, K.J., Mastrandrea, M.D., Bilir, T.E., Chatterjee, M., Ebi, K.L., Estrada, Y.O., Genova, R.C., Girma, B., Kissel, E.S., Levy, A.N., MacCracken, S., Mastrandrea, P.R., White, L.L. (Eds.), Climate Change 2014: Impacts, Adaptation, and Vulnerability. Part A: Global and Sectoral Aspects. Contribution of Working Group II to the Fifth Assessment Report of the Intergovernmental Panel on Climate Change. Cambridge University Press, pp. 1–32.
Jain, S.K., Kumar, V., 2012. Trend analysis of rainfall and temperature data for India. Curr. Sci. 102, 37–49.
Kabo-Bah, A.T., Diji, C., Nokoe, K., Mulugetta, Y., Obeng-Ofori, D., Akpoti, K., 2016. Multiyear rainfall and temperature trends in the Volta river basin and their potential impact on hydropower generation in Ghana. Climate 4 (4), 49.
Kahya, E., Kalaycı, S., 2004. Trend analysis of streamflow in Turkey. J. Hydrol. 289 (1–4), 128–144, 2004.
Kendall, M.G., 1955. Rank Correlation Methods. Charles Griffin, London, UK, 1955.
Kendall, M.G., 1975. Rank Correlation Methods, fourth ed. Charles Griffin, London, UK, p. 272.
Kim, J.S., Choi, C.U., 2013. Impact of changes in climate and land use/land cover change under climate change scenario on streamflow in the basin. J. Korean Soc. Geospat. Informat. Science 21 (2), 107–116.
Knutti, R., Abramowitz, G., Collins, M., Eyering, V., Gleckler, P.J., Hewitson, B., Mearns, L.O., Stocker, T.F., Qin, D., Plattner, G.K., Tignor, M., 2010. Good practice guidance paper on assessing and combining multi model climate projections, IPCC working group I technical support unit. In: Meeting Report of the Intergovernmental

Panel on Climate Change Expert Meeting on Assessing and Combining Multi Model Climate Projections. University of Bern, Bern.
Kumar, N., Tischbeinb, B., Kuschec, J., Laux, P., Bege, M.K., Bogardi, J.J., 2017. Impact of climate change on water resources of upper Kharun catchment in Chhattisgarh, India. J. Hydrol.: Reg. Stud. 13, 189–207.
Li, Q., Chen, X., Luo, Y., Lu, Z.H., Wang, Y.G., 2015. A new parallel framework of distributed SWAT calibration. J Arid Land 7, 122–131, 2015.
Mann, H.B., 1945. Nonparametric tests against trend. Econometrica 13, 245–259.
Masui, T., Matsumoto, K., Hijioka, Y., Kinoshita, T., Nozawa, T., Ishiwatari, S., Kato, E., Shukla, P.R., Yamagata, Y., Kainuma, M., 2011. An emission pathway for stabilization at 6 Wm22 radiative forcing. Clim. Change 109, 59–76.
Mondal, A., Khare, D., Kundu, S., 2015. Spatial and temporal analysis of rainfall and temperature trend of India. Theor. Appl. Climatol. 122 (1–2), 143–158.
Monteith, J.L., 1965. Evaporation and environment, in the state and movement of water in living organisms. Symp. Soc. Exp. Biol. 19, 205–234, 1965.
Moriasi, D.N., Arnold, J.G., Liew, M. W. Van, Bingner, R.L., Harmel, R.D., Veith, T.L., 2007. Model evaluation guidelines for systematic quantification of accuracy in watershed simulations. Transact. ASABE 50 (3), 885–900.
Moriasi, D.N., Gitau, M.W., Pai, N., Daggupati, P., 2015. Hydrologic and water quality models: performance measures and evaluation criteria. T ASABE 58, 1763–1785.
Moss, R.H., Edmonds, J. A Hibbard, Manning, K.A., Rose, M.R., Van Vuuren, S.K., Carter, D.P., R Emori, T., Kainuma, S., Kram, M., Meehl, T., Mitchell, G.A., Nakicenovic, J.F.B., Riahi, N., Smith, K., Stouffer, S.J., Thomson, R.J., Weyant, A.M., Wilbanks, J.P., T. J., 2010. The next generation of scenarios for climate change research and assessment. Nature 463 (7282), 747–756.
Mutenyo, I., Nejadhashemi, P., Woznicki, S., Giri, S., 2013. Evaluation of SWAT performance on a mountainous watershed in tropical Africa. Hydrol. Curr. Res. s14 (1), 1–7.
Nash, J., Sutcliffe, J., 1970. River flow forecasting through conceptual models: Part I. A discussion of principles. J. Hydrol. 10 (3), 282–290.
Naveendrakumar, G., Vithanage, M., Kwon, H.-H., Iqbal, M.C.M., Pathmarajah, S., Obeysekera, J., 2018. Five decadal trends in averages and extremes of rainfall and temperature in Sri Lanka. Adv. Meteorol. 2018, 13. Article ID 4217917.
Neitsch, S.L., Arnold, J.G., Kiniry, J.R., Williams, J.R., 2005. Soil and Water Assessment Tool, Theoretical Documentation Version 2005. USDA Agricultural Research Service and Texa A&M Blackland Research Center, Temple, TX, USA.
Neitsch, S.L., Arnold, J.G., Kiniry, J.R., Williams Grassland, J.R., 2011. Soil and Water Assessment Tool Theoretical Documentation Version. Texas Water Resources Institute, Temple, TX, USA.
Niang, A., Amrani, F., Salhi, M., Grelu, P., Sanchez, F., 2014. Rains of solitons in a figure-of-eight passively mode-locked fiber laser. Appl. Phys. B 116 (3), 771–775.
Osima, V.S., Indasi, M., Zaroug, H.S., Endris, M., Gudoshava, H.O., Misiani, A., Nimusiima, R.O., Anyah, G., Otieno, B.A., 2018. Ogwang projected climate over the greater horn of Africa under 1.5 C and 2 C global warmingEnviron. Res. Lett. 13. Article 065004.
Patakamuri, S.K., Das, B., 2019. Trendchange: Innovative Trend Analysis and Time-Series Change point Analysis. The R project for Statistical Computing, Vienna, Austria.
Patakamuri, S.K., O'Brien, N., 2019. Modified MK: Modified Mann-Kendall Trend Tests. The R R Project for Statistical Computing, Vienna, Austria.
Peleg, N., Shamir, E., Georgakakos, K.P., Morin, E., 2014. A framework for assessing hydrological regime sensitivity to climate change in a convective rainfall environment: a case study of two medium-sized eastern Mediterranean catchments, Israel. Hessd 11, 10553–10592.
Penman, H.L., 1948. Natural evaporation from open water, bare soil, and grass. Proc. R. Soc. Lond. Ser. A Math. Phys. Sci. 193, 120–145.
Piani, C., Weedon, G.P., Best, M., Gomes, S.M., Viterbo, P., Hagemann, S., Haerter, J.O., 2010. Statistical bias correction of global simulated daily precipitation and temperature for the application of hydrological models. J. Hydrol. 395 (3-4), 199–215.
Priestley, C.H.B., Taylor, R.J., 1972. On the assessment of surface heat flux and evaporation using large-scale parameters. Monthly Weather Rev. 100 (2), 81–92.
R Core Team, 2017. R. A Language and Environment for Statistical Computing. R Foundation for Statistical Computing, Vienna, Austria.
Rajsekhar, D., Gorelick, S.M., 2017. Increasing drought in Jordan: climate change and cascading Syrian land-use impacts on reducing transboundary flow. Sci. Adv. 3, 1–16.
Rathjens, H., Bieger, K., Srinivasan, R., Chaubey, I., Arnold, J.G., 2016. CMhyd user manual. Available online: http://swat.tamu.edu/software/cmhyd/.
Rehman, S., 2012. Long-term wind speed analysis and detection of its trends using Mann-Kendall test and linear regression method. Arabian J. Sci. Eng. 38 (2), 421–437.
Repas, T., 2011. Obesity and dyslipidemia. South Dakota Medicine.
Riahi, K., Rao, S., Krey, V., Cho, C., Chirkov, V., Fisher, G., Kindermann, G., Nakicenovic, N., Rafaj, P., 2011. RCP 8.5: a scenario of comparatively high greenhouse gas emissions. Clim. Change 109, 33–57.
Richard Woodroofe & Associates, 1996. Omo-gibe River basin integrated development master plan study final Report Vol. VI Water Resources Surveys and Inventories, Ministry of Water Resources. A.A.
Rivas-Tabares, D., Tarquis, A.M., Willaarts, B., Miguel, Á. De., 2019. An accurate evaluation of water availability in sub-arid Mediterranean watersheds through SWAT: cega-Eresma-Adaja Agric. Water Manag. 212, 211–225.
Sachindra, D.A., Huang, F., Barton, A., Perera, B.J., 2014a. Statistical downscaling of general circulation model outputs to precipitation—part 1: calibration and validation. Int. J. Climatol. 34, 3264–3281.
Sachindra, D.A., Huang, F., Barton, A., Perera, B.J., 2014b. Statistical downscaling of general circulation model outputs to precipitation—part 2: bias correction and future projections. Int. J. Climatol. 34, 3282–3330.
Saeed, F.H., Al-Khafaji, M.S., Al-Faraj, F., 2022. Hydrologic response of arid and semi-arid river basins in Iraq under a changing climate. J. Water Clim. Change 13 (3), 1225–1240.
Saha, P.P., Zeleke, K., 2015. Rainfall-Runoff modelling for sustainable water resources management: SWAT model review in Australia. In: Sustainability of Integrated Water Resources Management. Springer, Cham, pp. 563–578.
Salarijazi, M., Akhond-Ali, A.-M., Adib, A., Daneshkhah, A., 2012. Trend and change-point detection for the annual stream-flow series of the karun river at the Ahvaz hydrometric station. Afr. J. Agric. Res. 7, 4540–4552.
Samuels, R., Hochman, A., Baharad, A., Givati, A., Levi, Y., Yosef, Y., Saaroni, H., Ziv, B., Harpaz, T., Alpert, P., 2018. Evaluation and projection of extreme precipitation indices in the Eastern Mediterranean based on CMIP5 multi-model ensemble. Int. J. Climatol. 38 (5), 2280–2297.
Santhi, C., Arnold, J.G., Williams, J.R., Dugas, W.A., Srinivasan, R., Hauck, L.M., 2001. Validation of the SWAT model on a large river basin with point and nonpoint sources. J. Am. Water Resour. Assoc. 37, 1169–1188.
Seager, R., Ting, M., Li, C., Naik, N., Cook, B., Nakamura, J., Liu, H., 2013. Projections of declining surface-water availability for the southwestern United States. Nat. Clim. Change 3, 482–486.
Setegn, S.G., Srinivasan, R., Melesse, A.M., Dargahi, B., 2010. SWAT model application and prediction uncertainty analysis in the Lake Tana Basin, Ethiopia. Hydrol. Process. 24, 357–367.
Shamir, Eylon, Megdal, Sharon B., Carrillo, Carlos, Castro, Christopher L., Chang, Hsin-I, Chief, Karletta, Corkhill, Frank E., Eden, Susanna, Georgakakos, Konstantine P., Nelson, Keith M., Prietto, Jacob., 2015. Climate change and water resources management in the upper Santa Cruz river, Arizona. J. Hydrol. 521, 18–33.
Shi, X. P. Chen, Ma, X., Qu, S., Zhang, Z., 2013. Analysis of variation trends in precipitation in an upstream catchment of Huai river. Math. Probl Eng. 2013, 2013. Article ID 929383, 11 pages.
Shrestha, S., Bhatta, B., Shrestha, M., Shrestha, P.K., 2018. Integrated assessment of the climate and landuse change impact on hydrology and water quality in the Songkhram River Basin, Thailand. Science of the Total Environment 643, 1610–1622.
Singh, V., Bankar, N., Salunkhe, S.S., Bera, A.K., Sharma, J.R., 2013. Hydrological stream flow modelling on Tungabhadra catchment: parameterization and uncertainty analysis using SWAT CUP. Curr. Sci. India 104, 1187–1199.
Solomon, S.D., Qin, D., Manning, M., Chen, Z., Marquis, M., Averyt, K., et al., 2007. Climate Change, 2007. The Physical Science Basis Contributions of Working Group I to the Fourth Assessment Report of the Intergovernmental Panel on Climate Change. Cambridge University Press, Cambridge, United Kingdom, and New York, NY, USA.
Sood, A., Muthuwatta, L., McCartney, M., 2013. A SWAT evaluation of the effect of climate change on the hydrology of the Volta River basin. Water Int. 38 (3), 297–311.
Sorg, A., Bolch, T., Stoffel, M., Solomina, O., Beniston, M., 2012. Climate change impacts on glaciers and runoff in Tien Shan (Central Asia). Nat. Clim. Change 2 (10), 725–731.
Swain, J.B., Patra, K.C., 2019. Impact assessment of land use/land cover and climate change on streamflow regionalization in an ungauged catchment. J. Water Clim. Change 10 (3), 554–568.
Tan, M.L., Ficklin, D.L., Ibrahim, A.B., Yosup, Z., 2014. Impacts and uncertainties of climate change on streamflow of the Johor river basin, Malaysia using a CMIP5 general circulation model ensemble. J. Water Clim. Change 5 (4), 676–695.
Tapiador, F.J., Moreno, R., Navarro, A., Sánchez, J.L., García-Ortega, E., 2019. Climate classifications from regional and global climate models: performances for present climate estimates and expected changes in the future at high spatial resolution. Atmos. Res. 228, 107–121.
Taye, M.T., Dyer, E., Hirpa, F.A., Charles, K., 2018. Climate change impact on water resources in the Awash basin, Ethiopia. Water 10 (11), 1560.
Tayler, K.E., Stouffer, R.J., Meehl, G.A., 2012. An overview of CMIP5 and the 857 experimental design. Bull. Am. Meteorol. Soc. 858 93, 485–498.
Thomson, A.M., Calvin, K.V., Smith, S.J., Kyle, G.P., Volke, A., Patel, P., Delgado-Arias, S., Bond-Lamberty, B., Wise, M.A., Clarke, L.E., Edmonds, J.A., 2011. RCP 4.5: a pathway for stabilization of radiative forcing by 2100. Climatic Change 109, 77–94.
USDA-SCS, 1972. National Engineering Hanbook, Section 4–Hydrology. US Government Printing Office, Washington,DC, USA.
Van Vuuren, D.P., Den Elzen, M.G., Lucas, P.L., Eickhout, B., Strengers, B.J., Van Ruijven, B., Wonink, S., Van Houdt, R., 2007. Stabilizing greenhouse gas concentrations at low levels: an assessment of reduction strategies and costs. Climatic Change 81 (2), 119–159.
Van Vuuren, D.P., Stehfest, E., den Elzen, M.G.J., Kram, T., van Vliet, J., Deetman, S., Isaac, M., Goldewijk, K.K., Hof, A., Beltran, A.M., Oostenrijk, R., van Ruijven, B., 2011. RCP2.6: exploring the possibility to keep global mean temperature increase below 2 C. Climatic Change 109, 95–116.
Van Vuuren, D.P., Stehfest, E., den Elzen, M.G., Kram, T., van Vliet, J., Deetman, S., Isaac, M., Goldewijk, K.K., Hof, A., Beltran, A.M., Oostenrijk, R., 2011a. RCP2. 6: exploring the possibility to keep global mean temperature increase below 2 C. Climatic Change 109 (1), 95–116.
Walton, D.B., Sun, F., Hall, A., Capps, S., 2015. A hybrid dynamical–statistical downscaling technique. part I: development and validation of the technique. J. Clim. 28 (12), 4597–4617.
Wilby, R.L., Wigley, T.M.L., 1997. Downscaling general circulation model output: a review of methods and limitations. Prog. Phys. Geogr. 21, 530–548.
Wilby, R., Charles, S., Zorita, E., Timbal, B., 2004. Guidelines for use of climate scenarios developed from statistical downscaling methods. In: Supporting Material of the Intergovernmental Panel on Climate Change. Available from the DDC of IPCC TGCIA 27.
William, J.R., 1969. Flood routing with variable travel time or variable storage coefficients. Trans. ASAE (Am. Soc. Agric. Eng.) 12, 100–103.

Wise, M., Calvin, K., Thomson, A., Clarke, L., Bond-Lamberty, B., Sands, R., Smith, S.J., Janetos, A., Edmonds, J., 2009. Implications of limiting CO2 concentrations for land use and energy. Science 324 (5931), 1183–1186.
Worku, F.F., Werner, M., Wright, N., Zaag, P., Demissie, S.S., 2014. Flow regime change in an endorheic basin in southern Ethiopia. Hydrol. Earth Syst. Sci. 18 (9), 3837–3853.
Worku, G., Teferi, E., Bantider, A., Dile, Y.T., 2021. Modelling hydrological processes under climate change scenarios in the Jemma sub-basin of upper Blue Nile Basin, Ethiopia. Clim. Risk Manag. 31, 100272.
Wu, H., Chen, B., 2014. Evaluating uncertainty estimates in distributed hydrological modeling for the Wenjing River watershed in China by GLUE, SUFI-2, and ParaSol methods. Ecol. Eng. 76, 110–121, 2015.
Wu, Y., Liu, S., Abdul-Aziz, O.I., 2012. Hydrological effects of the increased CO2 and climate change in the Upper Mississippi River Basin using a modified SWAT. Clim. Chang 110 (3–4), 977–1003.
Xuan Hoan, Nguyen, Khoi, Dao Nguyen, Nhi, Pham Thi Thao, 2020. Uncertainty assessment of streamflow projection under the impact of climate change in the Lower Mekong Basin: a case study of the Srepok River Basin, Vietnam. Water Environ. J. 34 (1), 131–142, 2020.
Yang, K., Wu, H., Qin, J., Lin, C., Tang, W., Chen, Y., 2014. Recent climate changes over the Tibetan Plateau and their impacts on energy and water cycle: a review. Global Planet. Change 112, 79–91.
Yang, X., Wood, E.F., Sheffield, J., Ren, L., Zhang, M., Wang, Y., 2018. Bias correction of historical and future simulations of precipitation and temperature for China from CMIP5 models. J. Hydrometeorol. 19 (3), 609–623.
Zhang, H., Huang, G.H., Wang, D., Zhang, X., 2011. Multi-period calibration of a semi-distributed hydrological model based on hydroclimatic clustering. Adv. Water Resour. 34 (10), 1292–1303.